Facies analysis of a glaciomarine sequence, the Neotproterozoic Mirbat Sandstone Formation, Sultanate of Oman

Autor(en): **Kellerhals, Philipp / Matter, Albert**

Objekttyp: **Article**

Zeitschrift: **Eclogae Geologicae Helvetiae**

Band (Jahr): **96 (2003)**

Heft 1

PDF erstellt am: **22.09.2024**

Persistenter Link: https://doi.org/10.5169/seals-169006

0012-9402/03/010049-22
DOI 10.1007/s00015-003-1068-3
Birkhäuser Verlag, Basel, 2003

Eclogae geol. Helv. 96 (2003) 49–70

Facies analysis of a glaciomarine sequence, the Neoproterozoic Mirbat Sandstone Formation, Sultanate of Oman

PHILIPP KELLERHALS & ALBERT MATTER

Key words: Sedimentology, glaciation, facies, Mirbat Formation, Neoproterozoic, Oman

ABSTRACT

The Lower Member of the Mirbat Sandstone Formation in southern Oman represents an example of those enigmatic low-latitude Neoproterozoic glacial successions which have been taken as evidence for a "snowball Earth". The member is made up of a >400 m thick sequence of glacial and associated sedimentary rocks. Evidence for a glacial origin comes from surfaces with glacial striations, dropstones and diamictites containing striated and glacially shaped clasts, which deform underlying layers. Facies analysis reveals six depositional systems formed by ten facies associations. Excellent exposure allowed the study of these facies in three dimensions and the development of a detailed picture of these strongly interfingering facies.

The surface of the underlying crystalline basement shows considerable relief, including a valley system which is covered at its base by fluvial deposits and sediments of non-glacial scree facies. An approximately 120 m thick sequence of distal glaciomarine deposits consisting mainly of two rain-out diamictites follows. These are covered by terminoglacial deltaic deposits. The middle part of the Lower Member comprises deposits of proximal glaciomarine-, subglacial- and ice front deposits. The proximal glaciomarine deposits consist of strongly interfingering sediments of rain-out diamictites, turbidites and bottom-current channel fills. Intercalated into the proximal glaciomarine deposits are horizons of subglacial deposits indicated by marine glacial tunnelmouth deposits, glacial striations, fluviatile channel fill deposits from the ice front and stromatolitic limestones. The upper part of the Lower Member is again dominated by a ca. 200 m thick third rain-out diamictite from a distal glaciomarine environment. It is overlain by a regionally persistent stromatolitic limestone showing a strongly negative carbon isotopic signature characteristic of cap carbonates.

This succession leads to a general facies model for temperate, low latitude glaciomarine sediments deposited in a tectonically active horst-graben system during the break up of the late Proterozoic supercontinent. The synchronous deposition of glacial, fluvial and glaciomarine sediments reveals a dynamic glacial environment and a vigorous hydrological cycle. Therefore the Neoproterozoic oceans can not have been totally frozen as postulated by the snowball Earth hypothesis.

ZUSAMMENFASSUNG

Das untere Member der Mirbat Sandstein Formation im Dhofar (Südoman) repräsentiert eine der enigmatischen neoproterozoischen glazigenen Abfolgen deren Paläobreite und Fazies auf die Existenz von Gletschern auf Meereshöhe nahe dem Aequator hinweisen. Das Member besteht aus >400 m vorwiegend glaziomarinen klastischen Sedimenten. Diamiktite mit gekritzten Komponenten, typische glaziale Geschiebeformen und die liegende Lagen deformierenden „dropstones" sowie Oberflächen mit glazialen Schrammen sind untrügliche Merkmale eines glazialen Ablagerungsmilieus. Grosse lithologische Vielfalt und abrupte Wechsel von Korngrösse, Textur und sedimentären Strukturen kennzeichnen die komplexe Abfolge. Es konnten mittels Faziesanalyse sechs Ablagerungs-Systeme bestehend aus zehn Fazies-Assoziationen unterschieden werden.

Die kristalline Unterlage weist beträchtliches Relief auf mit Tälern, deren Basis lokal wenige Meter mächtige fluviatile Sedimente und grobblockiger Hangschutt auflagern. Darüber folgen zwei distale Diamiktite mit einer Gesamtmächtigkeit von mindestens 120 m, welche von glaziodeltaischen Sedimenten vom Gilbert Delta Typ überlagert werden. Der mittlere Teil des unteren Members besteht aus proximalen glaziomarinen und subglazialen Bildungen sowie fluviatilen Rinnensandsteinen, die vor der Eisfront abgelagert worden sind. Die proximalen glaziomarinen Sedimente stellen eine Wechselfolge sich lateral stark verfingernder Diamiktite, Turbidite und subaquatischer Rinnensandsteine dar. Darin eingeschaltet wurden vereinzelt subglaziale Horizonte nachgewiesen u.a. Flächen mit glazialen Schrammen und grobklastische Eistunnel Ablagerungen. Der obere Teil des unteren Members wird von einem dritten ca. 200 m mächtigen Diamiktit dominiert, der von einem stromatolitischen Kalk ("cap carbonate") überlagert wird.

Die detaillierte Faziesanalyse und die dreidimensionalen Aufschlussverhältnisse ermöglichen die Rekonstruktion eines generellen Faziesmodells für glaziomarine Sedimente, die in niedriger Breite in einem tektonisch aktiven Horst-Graben System während des Auseinanderbrechens des spätproterozoischen Superkontinents abgelagert worden sind. Die synchrone Ablagerung glazialer, fluviatiler und mariner Faziestypen weist auf ein dynamisches glaziales Milieu im Einflussbereich temperierter Gletscher sowie auf einen aktiven hydrologischen Zyklus. Die neoproterozoischen Meere können demnach nicht total von Eis bedeckt gewesen sein wie dies die Hypothese einer "snowball" Erde postuliert.

Institut für Geologie, Universität Bern, Baltzerstrasse 1, CH-3012 Bern, Switzerland
Corresponding author: Prof. Dr. A. Matter, Institut für Geologie, Universität Bern, Baltzerstrasse 1, 3012 Bern, Switzerland. E-mail: albert.matter@geo.unibe.ch

Introduction

Glacially derived sediments found on the Arabian Peninsula have long drawn the attention of geologists. Most work has been carried out on sediments of the Palaeozoic Gondwana glaciations. In Oman these are the Permo-Carboniferous Al Khlata Formation sediments of the Huqf-Haushi area (Gorin et al. 1982; Levell et al. 1988; Wright et al. 1990). In Saudi Arabia and Yemen, the Permo-Carboniferous glaciations resulted in the sediments of the Wadjid Formation (Helal 1964; McClure 1978; 1980) and the Akbra Shales (Kruck & Thiele 1983) respectively. The late Ordovician glaciation is represented in Saudi Arabia by the Zarqa and the Sarah Formations (Vaslet 1990) that form part of the Tabuk Formation of McClure (1978) and in Jordan by the Ammar Formation (Abed et al. 1993) .

In contrast to the above mentioned Palaeozoic glacial deposits, the Mirbat Sandstone Formation is unfossiliferous. It has been attributed to the Permo-Carboniferous based on a K-Ar age of 390–350 Ma of an altered basic dyke in the underlying crystalline basement (Qidwai et al. 1988). However, a Rb-Sr combined isochron, using rhyolite clasts from the Lower Member of the Mirbat Sandstone Formation and rhyolites in the Huqf area gave an age of 554±10 Ma (Platel et al. 1992; Kramers pers. comm. 1992). Based on this late Neoproterozoic age the Mirbat Sandstone Formation has been tentatively correlated by Loosveld et al. (1996) with the Abu Mahara Group in the Huqf and the Jabal Akhdar. Several glacial diamictites occur in the Ghubrah and Fiq Member of the Abu Mahara Group in the Jabal Akhdar region (Brasier et al. 2000) that are tentatively attributed by Leather (2001) to two glacial periods at 760–700 Ma and 600–500 Ma, respectively.

However, the Rb-Sr age and the correlations based upon it, as well as the correlation of late Neoproterozoic glaciations in general, remain controversial because they are still poorly constrained in time (Evans 2000). Although the age of the Mirbat Sandstone Formation is not precisely known, it is younger than the Leger granite and the Mirbat granodiorite. They are the only bodies cross-cutting the foliation of the metamorphic basement rocks and therefore represent the youngest intrusions in the area (Mercolli, pers. comm. 2002, Platel et al. 1992). The Leger granite has been dated 723±2 Ma using U-Pb zircon geochronology (Bowring and Worthing pers. comm. 2001). The emplacement of the Mirbat granodiorite was dated by Gass et al. (1990) at 706±40 Ma. Thus the Mirbat Sandstone Formation may indeed correlate with one of the glacials in the Jabal Akhdar.

Glacigenic successions are known from all continents and are found either along active, compressional plate margins or extensional plate margins (see Eyles 1993 for summary). In active margin settings, successions of turbidites and glacially influenced as well as volcaniclastic mass flows dominate. Along passive margins glacially-influenced, mostly marine strata are found. The deposits of the Lower Member of the Mirbat Sandstone Formation are clearly of glaciomarine origin and were deposited at the border of the Abu Mahara rift basin. They belong, therefore, to the passive plate margin type deposits (Loosveld et al. 1996).

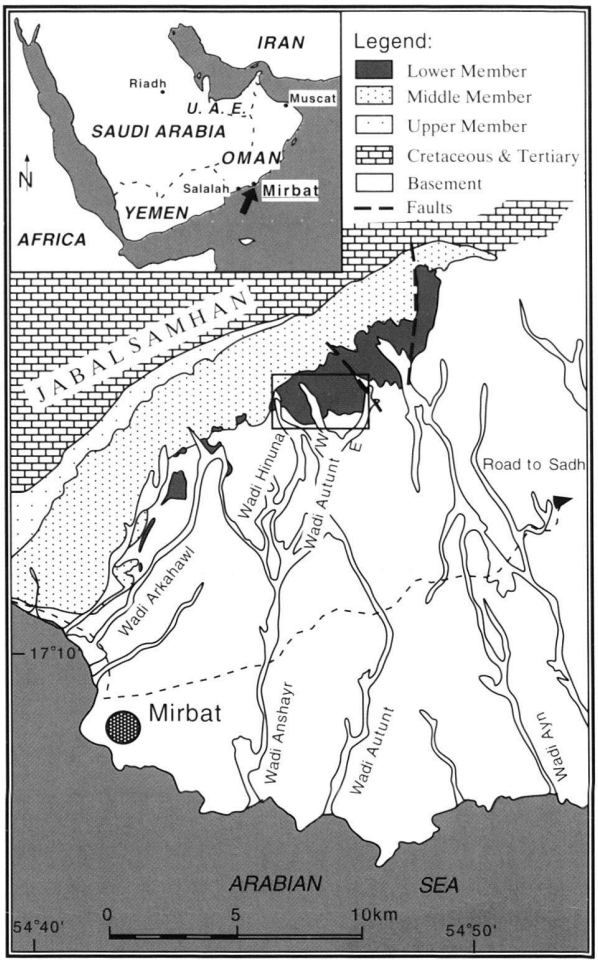

Fig. 1. Location map of the study area (rectangle) showing the outcrop area of the Mirbat Sandstone Formation.

Late Neoproterozoic glacial deposits, many of which record low-latitude glaciations, have recently gained an intense interest which has led to the snowball Earth hypothesis (Kirschvink 1992, Hoffman et al. 1998, Hoffman & Schrag 2002). This paper aims to provide a detailed sedimentological analysis of a Neoproterozoic glacial succession, the Lower Member of the Mirbat Sandstone Formation, focussing on lithofacies and facies associations in order to reconstruct the three dimensional depositional environment. Due to nearly three dimensional outcrop situation and lack of vegetation this area offers a superb opportunity to address these issues. The new findings may also add to the discussion on the snowball Earth hypothesis. First, we document the different lithofacies. Second, we discuss the nature of the depositional envi-

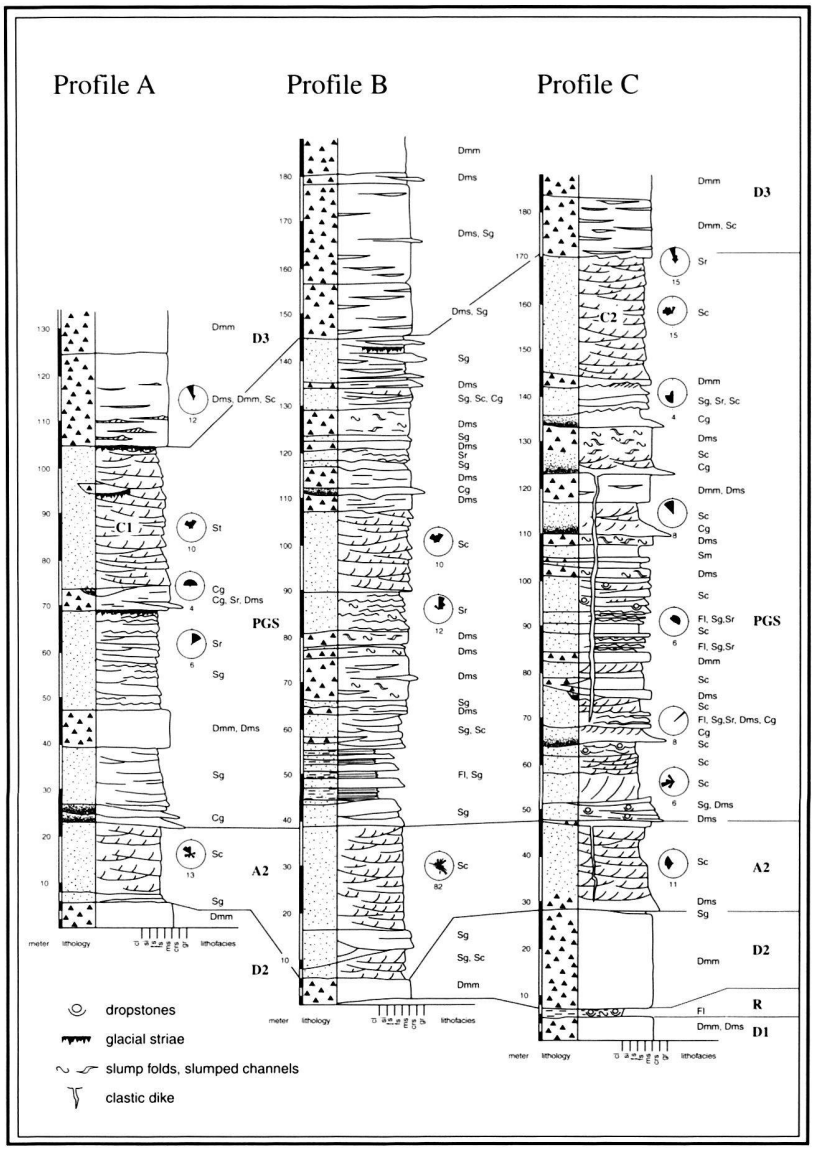

Fig. 2. Representative stratigraphic profiles of the proximal glaciomarine system. For location of profiles see Fig. 3. Lithofacies codes are as in Table 1, Facies association codes as in Table 2. Note that only the large-scale facies associations can be correlated (D1-3, A2).

ronments and then third, we develop a general facies model of this complex depositional setting. This is the first detailed description of a Neoproterozoic glaciation on the Arabian Peninsula.

Geological setting

The Mirbat Sandstone Formation crops out approximately 80 km NE of Salalah, NE of the town Mirbat in the southern part of the Sultanate of Oman (Fig. 1). It covers an area of about 100 km^2 and rests unconformably on crystalline basement (Mirbat granodiorite complex, Sadh- and Juffah gneisses (Würsten 1994; Briner 1997). The Mirbat Sandstone is itself unconformably overlain by Cretaceous and Tertiary sediments that form the Jabal Samhan (Fig. 1). The Mirbat Sandstone Formation dips to the NW at 8–10° and is divided into three Members: Lower (Ayn), Middle (Arkahawl) and Upper (Marsham) (Qidwai et al. 1988) . This paper focuses on the Lower Member which was mapped in detail by Kleiber (1993) . It is dominated by glacial sediments that crop out over a 20 km wide area with a surface of around 20 km^2 and a thickness of more than 400 m. A fetid stromatolitic limestone forms the top of the Lower Member.

The general transport direction of the Mirbat Sandstone Formation is towards the North-West, approximately into the southernmost end of the Abu Mahara Basin (Loosveld et al. 1996, Kellerhals, 1993, 1998). Thus the outcrop region is located at the eastern flank of a marine rift basin that was active in the Late Proterozoic (580–530 Ma) according to Loosveld et al. (1996).

Table 1. Description of lithofacies and interpretation of the sedimentation processes.

Litho-facies	Description	Interpretation
Bg	**Graded breccias:** thickly bedded clast-supported breccia with clasts up to 0.5 m. The purple matrix is silt- to sand-rich and the poorly sorted clasts come from the underlying crystalline basement (Sadh-, Juffah-Gneisses). Mostly the beds show a lateral extension of tens to hundreds of meters. Small stringers or channels of Bg can also be found.	The clast size and the fine to medium grained matrix indicate deposition by a mudflow.
Cg	**Graded conglomerates:** thin to thick beds of normally-graded, poorly-sorted, clast-supported conglomerates. The matrix is a coarse sandstone and the clast size can be up to 30 cm. Most beds have an erosive base and a lens-like shape with a lateral extension of several to several hundreds of meters. Often they are amalgamated forming units up to 5 m thickness. Rarely also matrix supported Cg can be found with clasts up to 1m diameter.	The graded clast-supported conglomerate beds are the product of turbulent high energy traction currents.
Dcm	**Massive clast-rich diamictite:** with angular clasts of up to 2 m in diameter and a silty matrix of purple colour. All the clasts derive from the underlying basement (Fig. 4a).	Formed by debris flow or rockfall processes.
Dmm	**Massive matrix-supported diamictite:** the Dmm are massive with little internal organisation or structure and have a brown or purple colour (Fig. 4c). Bed thickness varies from thin to very thick (>40m). Their lateral extension ranges from tens of meters to kilometers. The scattered angular to subrounded clasts of up to 50 cm show no preferred long axis alignment and a variable concentration in the silt or sand matrix. The clasts show striations along the long axis and they have often a bullet- or flat-iron shape (Fig. 4b).	The striated clasts with their (glacially formed) shapes (Fig. 4b) indicate a glacial origin. According to Eyles et al. (1993), massive diamictites (Dmm) are deposited in a wide range of glaciogenic environments by different processes, such as subglacial deformation and lodgement, subaqueous and subaerial resedimentation and subaqueous rain-out of suspended sediments and ice-rafted debris. A specific interpretation of this facies can only be given, if the shape of the bed and the interfingering with other lithofacies is taken into account (Dreimanis, 1979) .
Dms	**Stratified matrix-supported diamictite:** same as Dmm, but more than 10% of the diamictite shows a stratification consisting of stringers and channels of gravels or intercalations of sandy/silty layers. The maximum clast size is usually smaller than in the Dmm and clast long axes are mostly aligned parallel to the bedding plane in a keel downward position (Fig. 4d).	The stratified diamictites (Dms) resemble very much tillites sensu stricto. The clast rich beds are typical deposits of the ice marginal zones, caused by small mass- and grain-flows. The other possibility is a combination of rain-out into a traction current. Resedimented diamictites can form also Dms. Again one can define the deposition process only after examination of the bedforms and the surrounding sediments.
Sg	**Graded sandstones:** mostly orange or ochre coarse- to medium-grained, normal graded sandstones with an erosive base. In the upper part of the coarser Sg rip up clasts are frequent with sizes up to 5mm. The thickness of the individual beds varies from several decimeters to several meters and the lateral extension ranges from several tens to hundreds of meters. The beds are often amalgamated.	Deposition by waning turbulent current. Generally Ta division of turbidites.

Sc	**Cross-bedded sandstones:** medium- to coarse - grained, orange to ochre sandstones showing trough or tabular crossbedding. The single sets measure from several decimetres up to 15 m. The beds have an erosive base and a lens-like geometry. Often associated with Sc are oversized clasts (<60 cm diameter). There is also a brown variety of Sc. The set heights are in the range of dm, but often superimposed sets are more than 5-12 m high. This sandstone looks like the 'matrix' of the Dmm with a high clay content and some larger feldspar grains with a size of up to 1 mm.	The trough and tabular cross-beds reveal deposition under undirectional currents and straight crested to sinuous bedforms, migrating dunes respectively.
Sr	**Rippled sandstones:** fine-to medium-grained orange to ochre sandstones showing mostly straight crested, rarely bifurcated, asymmetric ripples. Climbing ripples are also present. The amplitude (h) is less than 1 cm and the wave length is around 10 cm. Bed thickness varies from several cm to several decimeters.	The erosive contacts of the discrete beds suggest bed load transport caused by a unidirectional current. The rarely seen bifurcated crests may be a sign of slight wave action. Possible unidirectional palaeocurrents could be storm-surge ebb or wind driven currents.
Sl	**Laminated sandstones:** thin- to thick-laminated orange to ochre sandstones made up of alternating fine to medium, rarely coarse grained laminae.	The normal grading and the parallel lamination suggest deposition from suspension for the fine-to medium-grained sandstones and/or deposition as bed load transport by traction currents for the coarse -grained (>0.6 mm) sandstones (Tucker, 1986) .
Fl	**Laminated siltstones:** fine to medium-grained parallel laminated dark brown, purple or grey siltstones. Slightly wavy lamination is sometimes present. Stringers of coarser grained sands are common. Bed thickness varies from several centimeters to several meters (Fig. 6d).	Deposition from suspension (background sedimentation) or low energy current.
Lg	**Graded silty limestones:** slightly undulous beds of 0.1-15 cm thickness showing a fining upward trend of their silt/intraclast content. The matrix is a microsparite which shows strongly negative $\delta^{13}C$ values.	The internal grading of these limestones is indicative of turbidity currents.
Ls	**Stromatolitic limestones:** laminated undulous beds of varying thickness (0.5-8 mm) with colours ranging from grey, brown, red to white. Large scale domal buildups of up to 1m diameter are also found. The laminae are formed by micrite/microsparite with intercalations of sparitic interlayers and very few single grain silt layers. Some areas are organic rich with a high pyrite content. Fenestrae and wavy-crinkly lamination may be also present. Rare samples reveal cell-like spheres of 60 µm diameter (Fig. 5c). The undulous laminations are horizons of rounded intraclasts which are draped by the limestone laminae resulting in pustular/small scale domal build-ups. (Fig. 5a). Strongly negative $\delta^{13}C$ values.	These finely laminated limestones are of cyanobacterial origin.

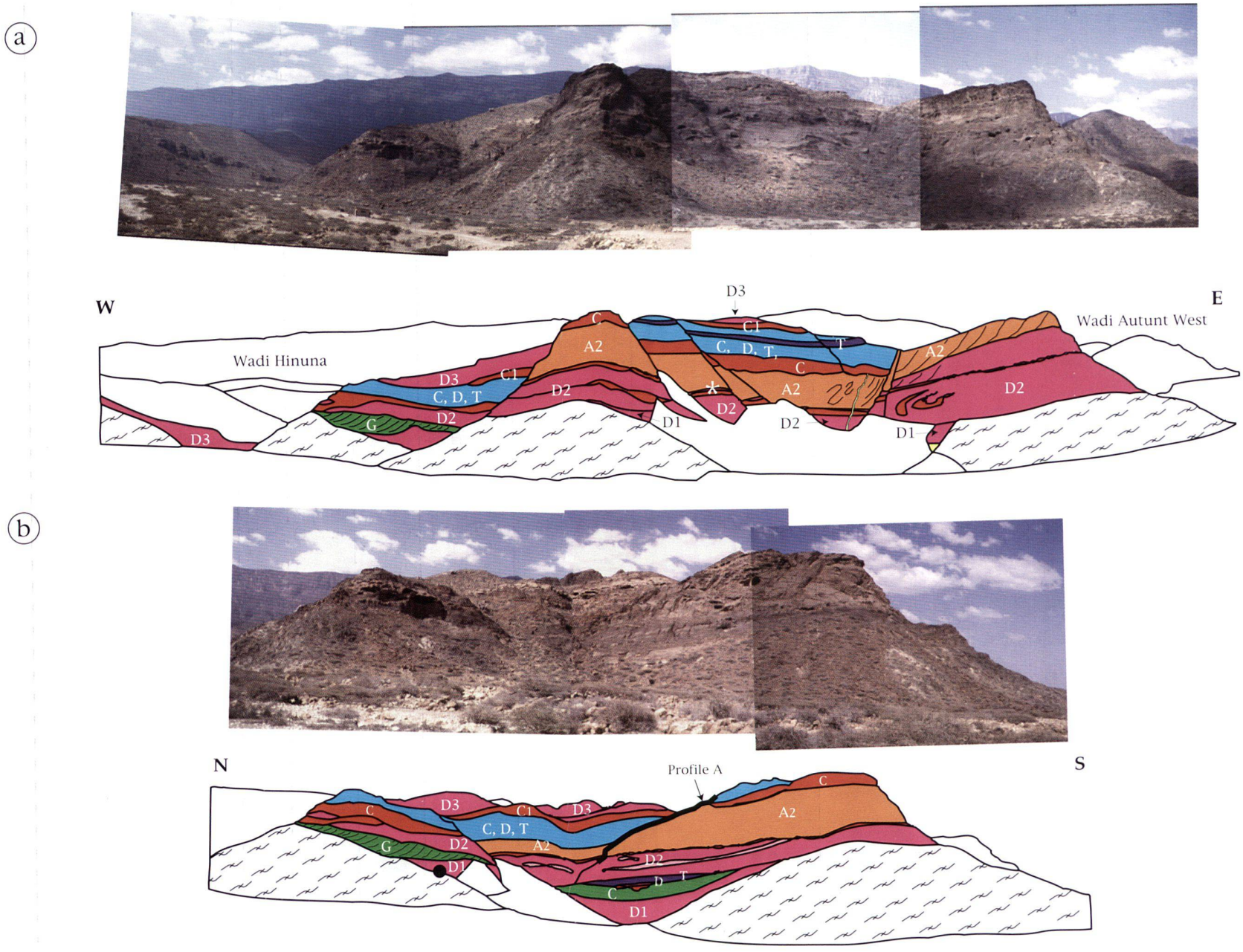
a
W
E
D3
Wadi Hinuna
Wadi Autunt West
C
A2
C1
C, D, T
D2
G
D1
b
N
S
Profile A

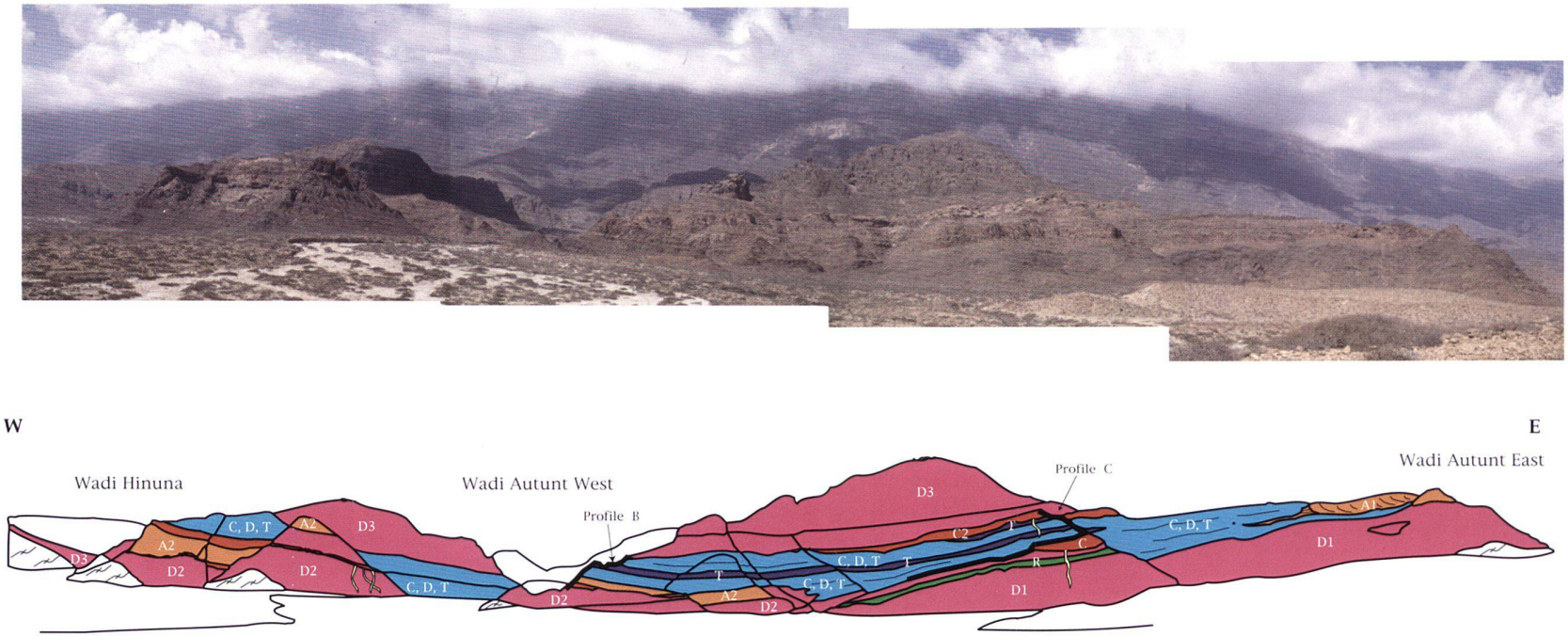

Fig. 3. Photopanoramas and interpretations of depositional systems and large-scale facies associations:
a) Wadi Autunt West (distance from left to right 800 m).
b) Entrance of Wadi Hinuna with outcrop of the Gilbert-type delta (G). (Distance from left to right 800 m).
c) Frontal view of the study area showing the distribution of facies associations in the Lower Member of the Mirbat Sandstone Formation. The sequence is dominated by distal facies at the base (D1) and at the top (D3) with dominantly proximal facies (C, D, T) in-between.

D: rain-out diamictite facies association, C: channel sandbody facies association (red), A1, A2: alternate bars of the fluvial facies association (orange), C1, C2: channels of the fluvial facies association (red), T: turbidite facies association (dark blue), R: rhythmites facies association (green), G: Gilbert delta facies association (green). C, D, T indicates areas were the facies associations of channel sandbody, rain-out diamictites and turbidites are intimately interfingering beyond the resolution (light blue). Scree facies association (yellow).

* marine glacial tunnel-mouth facies association (subaqueous esker), • Stromatolitic limestone of the limestone facies association. Distance from Wadi Hinuna to Wadi Autunt East is 4.5 km.

Table 2. Facies hierarchy with facies associations and their lithofacies elements. Abbreviations of the lithofacies elements are according to Table 1. The examples of facies associations listed are those shown in Figs 3 and 10.

Depositional systems	*Facies associations*	*Examples:*	*Lithofacies elements*
Distal glaciomarine system:	*Rain-out diamictite facies association :* *Channel sandbody facies association :* *Limestone facies association :*	*D1, D3*	*Dmm, Dms,* *Sg, Sr, Sc, Sh* *Ls, Lg, Sg*
Proximal glaciomarine system:	*Rain-out diamictite facies association :* *Channel sandbody facies association :* *Turbidite facies association :*	*D, D2* *C* *T*	*Dms, Dmm, Sg,* *Sg, Sr, Sc, Sh* *Sg, Sh, Sr, Fl,*
Terminoglacial deltaic system:	*Gilbert-type delta facies association :* *Rhythmite facies association :* *Limestone facies association:*	*G* *R*	*Sc, Fl, Sg* *Fl, (Sg)* *Ls, Lg,*
Subglacial system:	*Marine glacial tunnel-mouth facies association:* *Glacial striations facies association:*		*Cg, Dmm, Sg,* *Fl, Dms*
Ice front system:	*Fluvial facies association :*	*A1, A2;* *C1, C2*	*Sc, Sr, Sg, (Dms)*
Subaerial non glacial system:	*Scree facies association :*		*Dmc, Bg, Fl*

Lithofacies descriptions

To reconstruct a three dimensional facies model a tectonically undisturbed rectangular outcrop area with a length of 4.5 km and a width of 0.8 km was chosen based on the map of Kleiber (1993). Detailed stratigraphic analyses (Fig. 2) reveal the recurring appearance of individual lithofacies types. The general character of each lithofacies together with an environmental interpretation is summarised in Table 1. The codes of the lithofacies elements are according to Eyles et al. (1983). The facies associations follow the terminology of Boulton & Deynoux (1981), Brodzikowski & van Loon (1991) and Eyles (1993). The 3-D facies relationships and evolution were analysed with the help of three major photographic panoramas (Fig. 3), numerous photographs, drawings and detailed field observations.

Depositional systems

The Lower Member of the Mirbat Sandstone Formation is characterised by high lithological diversity including conglomerates, breccias, diamictites, sandstones and siltstones, consisting exclusively of detritus derived from the crystalline basement, and rare limestones. Moreover, marked vertical and lateral variations of grain-size, texture, sedimentary structure and bedding characteristics across bounding surfaces of lithological units are generally observed as well as frequent channeling. Using these facies criteria twelve lithofacies types are defined and briefly discussed in Table 1. Based on the analysis of lithofacies and facies associations the Lower Member is subdivided in this paper into six depositional systems. The facies hierarchy is shown in Table 2. In addition, code letters are used for individual facies associations that are large enough to be shown in Figure 3.

Distal glaciomarine system

Rain-out diamictite facies association

Description: This facies association is composed of more than 95% massive matrix-supported diamictites (Dmm) with abundant faceted and striated igneous clasts (Figs 4b,c) and rare stratified, matrix-supported diamictites (Dms, Fig. 4d). Generally, this facies association consists of crudely bedded and well cemented, generally >20 m thick sheet-like bodies with sharp non-erosive basal contacts and flat tops. They are frequently stacked, forming up to 200 m thick units (e.g. D1, D3 in Fig. 3). Incorporated into these thick bodies are sandstones of the channel sandbody facies association (see below). All the diamictites are grey-green and maroon with the exception of those overlying the crystalline basement (lowest part of D1). The latter are dark purple in colour and contain exclusively clasts from the underlying basement. In the stratified diamictites (Dms), dropstone structures produced by clasts of various sizes (2–50 cm diameter) are frequently observed deforming the underlying bedding as well as local slumps. The latter are also found in the associated rare channelised sandstones.

Interpretation: The tabular geometry and considerable thickness of the diamictite bodies together with their massive to weakly stratified nature indicate rapid rain-out sedimentation from icebergs or shelf ice as the main process with minor reworking by traction currents (Eyles et al. 1985). This interpretation is further supported by the observation of dropstones found in the Dms indicating a subaquatic environment. A mass flow origin of the massive diamictites is excluded on the basis of their sheet-like geometry and lack of any grading. There is no evidence of a subglacial origin of these deposits such as glacial striations or other subglacial features. The local source of the clasts in the lowest part of D1 indicates a short transport distance.

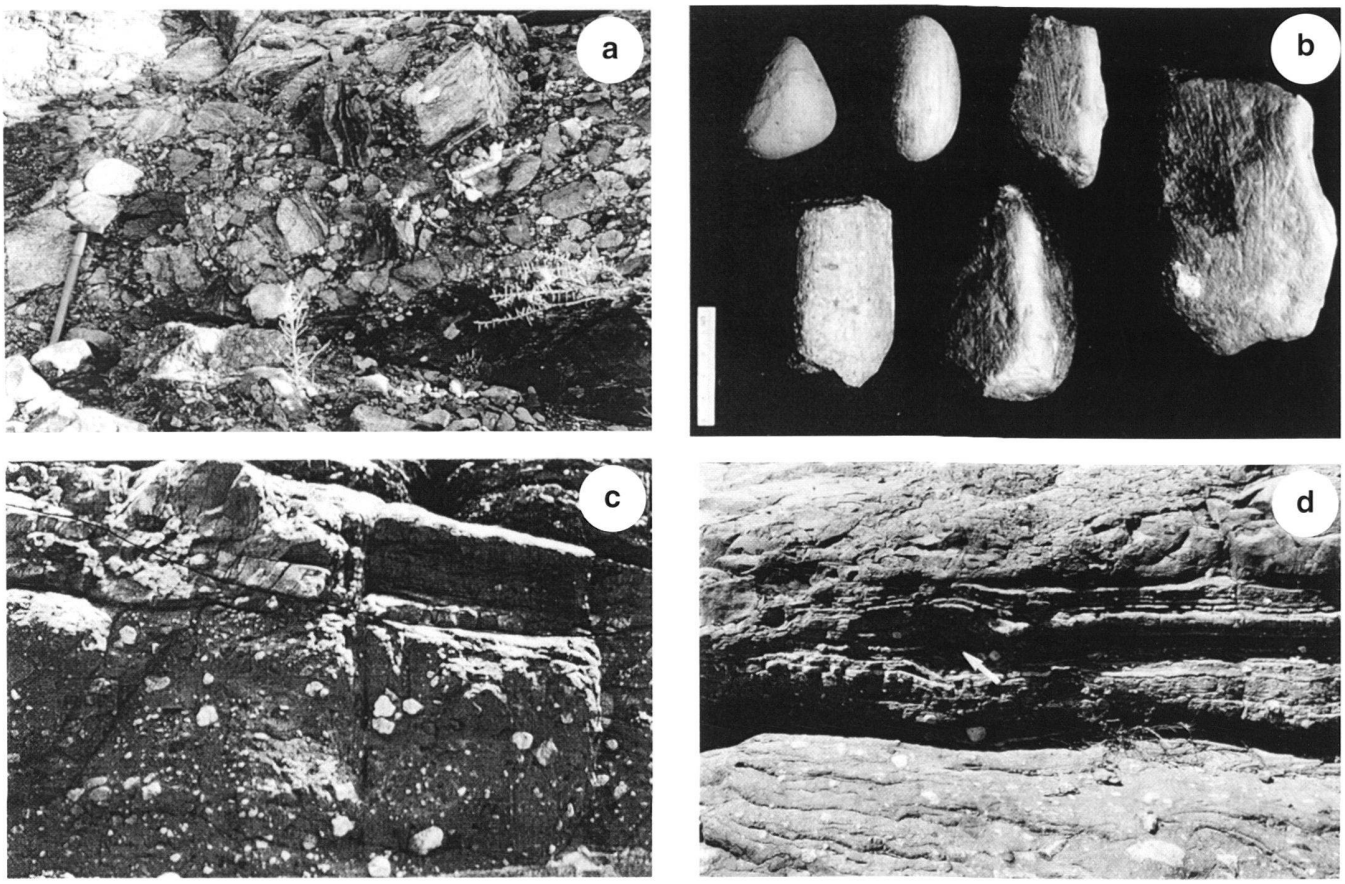

Fig. 4. Outcrop and clast photographs: a) Massive clast-supported diamictite (Dmc) of the scree deposits, b) Collection of striated glacially formed clasts, c) 2 m of massive matrix-supported diamictite (Dmm) with a channelised sandstone on top, d) Typical appearance of current reworked, stratified diamictite (Dms). Arrow points to the imprint of a dropstone (10 cm in diameter). The lower part of the diamictite is a massive matrix-supported (Dmm).

Channel sandbody facies association

Description: Flat lens-shaped ochre to orange coloured sandstone channel fills composed of clay-free arkose are generally found as isolated, randomly distributed bodies in the massive rain-out diamictites (Dmm). More rarely, vertical stacked channels separated by stratified rain-out diamictites (Dms), both commonly deformed by slumping, are also observed. They can be 0.1–3 m deep and 2–1000 m wide. The thicker ones (>1 m) represent multistorey sandbodies consisting mainly of well-sorted dune cross-bedded sandstones (Sc); the thinner beds, however, are graded sandstones (Sg).

Interpretation: The internal organisation of the sandstone channels which is dominated by dunes, the good sorting and their appearance in the rain-out diamictites suggests deposition from quasi-continuous subaquatic traction currents (see channel sandbody facies association of the proximal glaciomarine system). Minor turbidity current activity is indicated by the graded sandstones (Sg). The occurrence of clusters of channels suggests a long-lived sediment source, channelised flow and frequent avulsion within a laterally restricted belt. Continuous reworking occurred in the interchannel areas within this belt as indicated by the interbedded stratified diamictites (Dms). Because the massive rain-out diamictite surrounding the channel belt shows that the glacier reached the sea, these channel fills represent the distal deposits of a tunnel-mouth outlet (Brodzikowski & van Loon 1991). Clusters of channels record major tunnel-mouth outlets with greater longevity of position than isolated channels. Slumping and the origin of turbidites is attributed to oversteepening of the accumulated sediments possibly in combination with tectonic activity (Domack 1983; Eyles 1977; Eyles et al. 1985).

Limestone facies association

Description: Limestones associated with diamictites were observed both within the rain-out diamictites of D1 (Fig. 3b) and above the diamictite D3. The intra-diamicite limestone is laterally discontinuous and can be followed over less than about 20 metres before it comes to rest with unconformable contact on

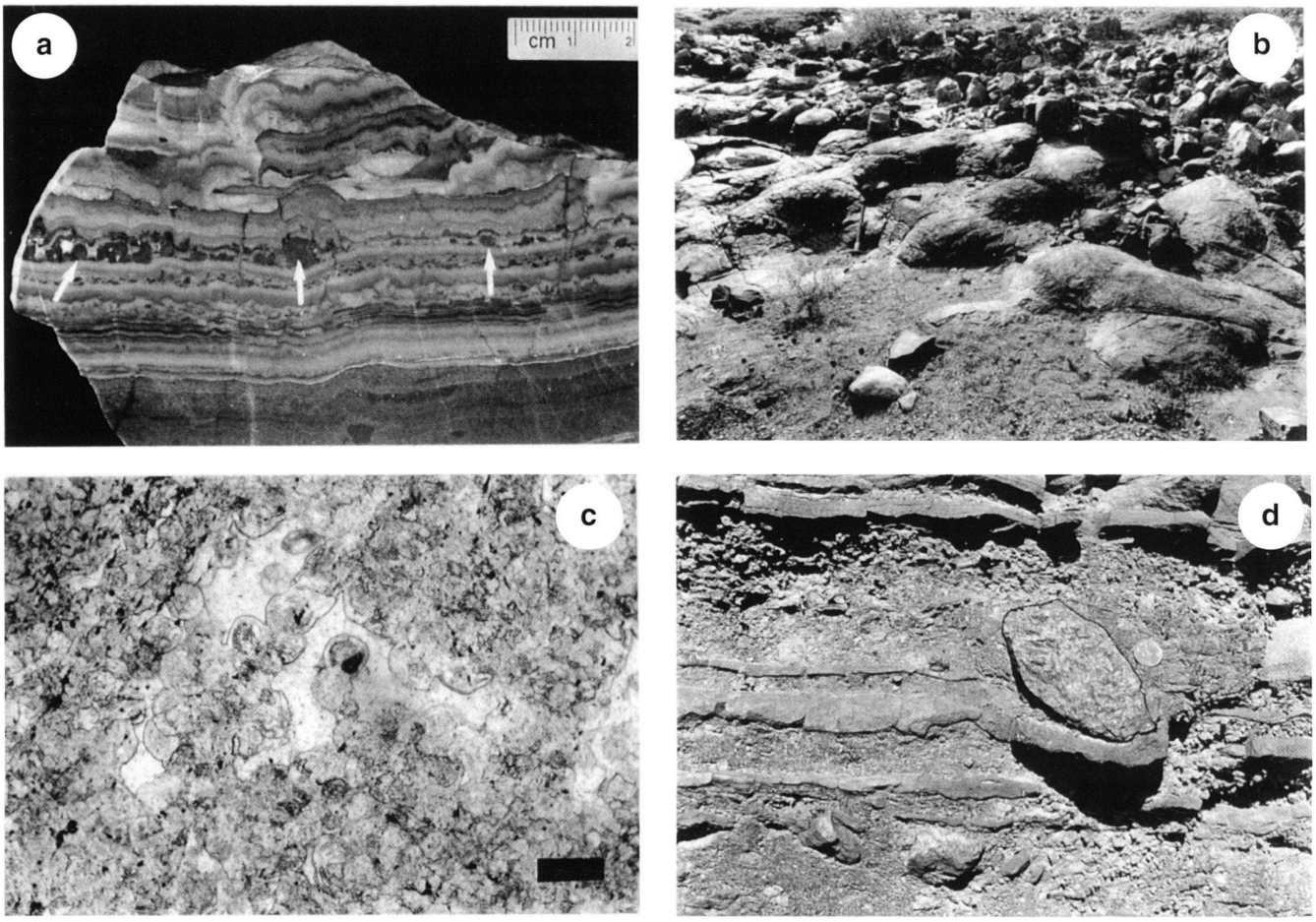

Fig. 5. Slab and outcrop photographs: a) Stromatolitic limestone found below the Gilbert delta (G) within facies association D1. Note the domal buildups formed by cohesive layers on top of rounded intraclasts (arrows). The lower part is dominated by calciturbidites (Lg). b) Large-scale domal stromatolites of fetid limestone overlying facies association D3. This limestone is equivalent to cap dolostones. c) Cell-like spheres of 60 m diameter forming colonies in fenestrae (scale bar = 0.1 mm). d) Silty graded limestone (Lg) bed deformed by a dropstone (coin is 1.5 cm).

the crystalline basement high (Fig. 3b). It consists of two beds measuring 5 and 30 cm respectively in thickness which are separated by a graded sandstone (Sg). The base of each bed is a finely laminated, organic free sparry limestone, which is overlain by numerous <1 cm thick graded silty limestone layers (Lg). These are followed by a stromatolitic limestone (Ls). Rare sand stringers composed of layers a single grain to a few grains in thickness are also observed (Fig. 5a). The $\delta^{13}C$ values of microbially laminated layers and silty limestone layers are almost identical ranging from –4.08‰ to –5.38‰.

The fetid limestone resting on the top of diamictite D3 is regionally persistent. It consists of a cm to dm thick finely laminated bed (Ls). Occasionally this bed shows domal structures of more than 1 m in diameter and up to 2.5 m height (Fig. 5b). Soft-sediment deformation structures are pervasive as well as intercalated, thin, graded silty to sandy limestone layers (Lg). In places the limestone is brecciated. Two types of cell-like slighty irregularly shaped spheres could be identified in one sample (Fig. 5c), the first with a diameter of 25–30 µm and a thin (3–6 µm) extracellular envelope. The second and larger with a diameter of 60 µm, includes sometimes dark granules which may represent remains of cell contents. Colonies of the second are abundant bordering larger spar-filled fenestrae. These spheres fluoresce when excited with UV light indicating the presence of organic matter. The $\delta^{13}C$ values of this limestone vary from –2.30‰ to –5.37‰. In one sample a few scattered small (<1cm) barite crystal fans were observed.

Interpretation: Although all the remains of these cells have undergone early diagenetic mineralisation, they may be interpreted as 'remains of colonial coccoid cyanobacterial unicells and/or capsules, sometimes coated with cement which may have precipitated within extracellular mucilaginous gel' (David

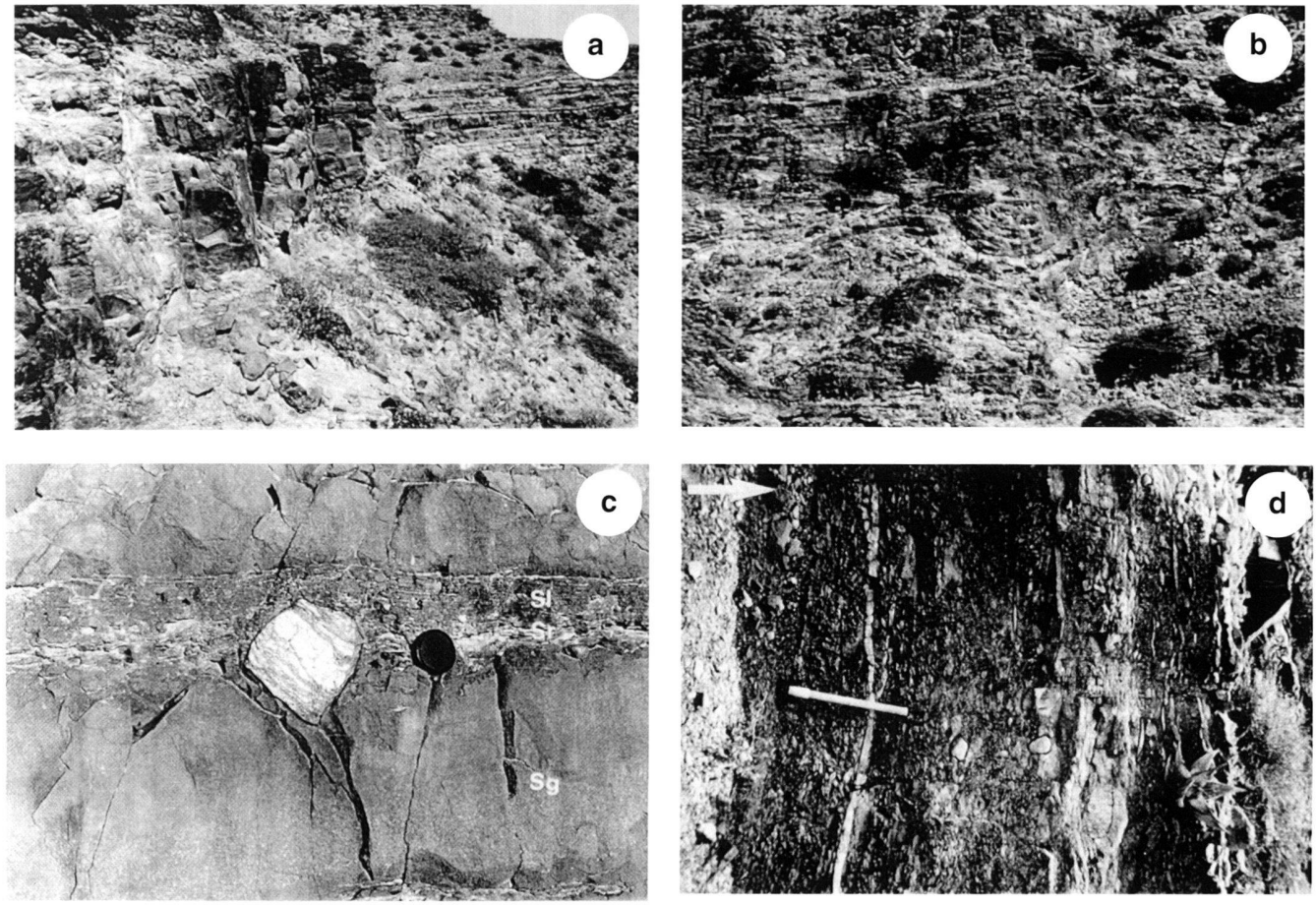

Fig. 6. Outcrop photographs: a) Channel sandbody facies of the proximal glaciomarine system (Channel is about 2m thick). b) U-shaped channel, 3m deep, eroded into a Dms. Note the wings formed by the infilling sandstones. c) Complete Bouma Ta-e sequence with dropstone in upper part (lens cap is 5 cm). d) Rhythmites with several dropstones. Number of small-scale sandstone channels increases towards the top (hammer = 60 cm, arrow points stratigraphically up).

Wright pers. comm. 1998). The cyanobacterial stromatolites grew in a low energy environment beyond the influence of waves to form their domal buildups. However, most of the limestone facies association is formed by graded silty to sandy limestones (Lg) deposited by turbidites. Obviously a relatively low energy environment allowing stromatolitic growth was interrupted from time to time by higher energy events, during which the stromatolitic limestones were partly eroded and the clasts redeposited by turbidity currents. This is supported by the identical strongly negative carbon isotope signature of both microbial layers and graded limestone layers. The many slumps are indicative of unstable slope deposition. Since the stromatolites where found within the rain-out diamictite facies association they might have grown in a glacial environment, but direct proof is missing in contrast to those found in the terminoglacial deltaic system described further below. The stromatolite bed above diamictite D3 is interpreted as a cap carbonate.

Proximal glaciomarine system

Channel sandbody facies association

Description: This facies association makes up 50–75% of the proximal glaciomarine deposits. The channel sandbody facies association (C) consists mainly of a clay-free, medium to coarse grained arkose which, due to the high feldspar content, is ochre to orange in colour. Both flat, lenticular multistorey (Fig. 6a) and highly erosive U-shaped (Fig. 6b) singlestorey channels are observed. The lenticular channels vary considerably in thickness from 0.3–15 m and in width from 15–>500 m. Channels thicker than 1 m are made up of several channel units with vertically stacked dune cosets (Sc), whereas the thinner ones (<1 m) are formed by graded sandstones (Sg). The wings of these multistorey bodies interfinger with the surrounding turbidite and rain-out diamictite facies associations. A thinning- and fining-upward trend is common, as is an erosive base. Outsized clasts ranging from 2–30 cm in diameter are abundant in the upper part of the smaller channels.

In contrast, the highly erosive, U-shaped channels, which are generally located on top of the large lenticular channels and rarely in the diamictites, are only 5–30 m wide and 3–10 m deep. Typically, the infilling graded sandstone (Sg) beds drape the steep channel walls and form wings extending laterally a few meters (Fig. 6b). Slumped beds and interbedded diamictite layers (Dms) are also present in the channel fill. The direction of the channel axes differs by up to 90° from the general flow direction observed in the Lower Mirbat Member (Fig. 2).

Interpretation: The generally symmetrical cross-section of both channel types and lack of lateral accretion suggests straight to slightly sinuous channel courses. The interfingering of multistorey channel deposits with rain-out diamictites and turbidites indicates a subaquatic glaciomarine depositional environment with an ice sheet reaching the sea. Due to the common occurrence of dunes in these channel infills they most likely formed under laminar traction currents representing meltwater underflow from tunnel-mouth outlets (Rust & Romanelli 1975). To produce an underflow of meltwater in sea water, the meltwater has to exceed the density of the sea water, which requires a suspended sediment concentration greater than 34 g l^{-1} (Mackiewicz et al. 1984). Although this is far more than observed in most recent meltwaters (~2 g l^{-1}), short term/catastrophic discharges (jökulhlaup) of large water masses are said to have enough suspended load to form underflows. In modern environments underflows are relatively uncommon, yet they appear to have occurred frequently in the Lower Member of the Mirbat Sandstone Formation. These meltwater currents are generally not continuous and may vary seasonally and diurnally (Church & Gilbert 1975), which may be one of the causes for the intimate interfingering of the three facies associations in this system. The dominance of the tunnel-mouth deposits indicates a proximal glaciomarine environment of all facies associations of this system. Minor turbidity current activity is indicated by the graded sandstones (Sg).

The highly erosive, U-shaped channels are interpreted as crevasse channels. This interpretation is supported by the divergent direction of the channel axis and their occurrence on the top of the large multistorey channels.

Rain-out diamictite facies association

Description: The rain-out diamictite facies association forms only about 25% of the proximal glaciomarine system. Crudely bedded sheet-like bodies of massive matrix-supported diamictites (Dmm) are mostly missing, whereas this facies association is characterised mainly by stratified matrix-supported diamictite (Dms) beds (Fig. 2, 4d) which were deposited in flat, lens-like channels with a width of more than 100 m and a depth of <10 m (D in Fig. 3a, b, c). These diamictites are always found either interbedded or laterally interfingering with the other facies associations of the proximal glaciomarine system. Incorporated in the Dms are numerous small-scale sandstone channel fills (0.1–5 m wide and 1–30 cm thick). Slumps are common in this facies association. In addition to the above mentioned diamictites a nearly 25 m thick body of massive matrix-supported diamictite (D2 in Fig. 3a, b, c) occurs in the west of the outcrop area. The eastern part of this body interfingers intimately with the other facies associations of the proximal glaciomarine system.

Interpretation: To interpret the depositional mechanism of these stratified diamictites one has to take into account the characteristics of the associated facies associations. The turbidites (see below) infer a subaqueous environment with a constant rain-out mechanism as shown by the numerous dropstones. Therefore the stratified matrix-supported diamictites (Dms) are deposited by rain-out from icebergs in combination with reworking by traction currents from tunnel-mouth outlets (described above in the channel sandbody facies association). The few up to 25 m thick matrix-supported massive diamictite (Dmm) beds formed by rain-out deposition in areas where tunnel-mouth outlets were absent.

Turbidite facies association

Description: Large channels with flat lens-like geometry and a thickness of 2–10 m and a lateral extension of 100–1000 m are intimately associated with the channel sandbody and rain-out diamictite facies associations. Two readily distinguishable channel types are developed, indicating different depositional processes. Fill of the first channel type consists of numerous small scale (0.7–2 m thick) channel bodies which overlap both vertically and laterally. This type of channel fill records a high lateral instability with short-term channel migrations. In contrast, fill of the second channel type is made up of stacked horizontal beds. In both channel types individual beds consist of complete Ta-e Bouma divisions. Rip-up clay particles are often observed in the upper part of the Ta interval. The ripples of interval Tc are asymmetric, often lunate with a wave length of around 10 cm. Climbing ripples are abundant and the general flow direction varies from NW to NE (see Fig. 2). Outsized clasts (dropstones) with a maximum diameter of 40 cm deforming the underlying bedding (Fig. 6c) are abundant in laminated siltstones of the Te division, whereas they are very sparse in the sandstone Ta-d divisions. Some thin (<40 cm) Dmm beds are found interbedded with the sandstones.

Interpretation: The turbidites were deposited in flat shallow channels by numerous pulses of turbiditic events. During the pauses between consecutive turbidites, deposition of background sediment from rain-out of icebergs is documented by intercalations of Dmm beds and dropstones. This, together with the dominance of complete Bouma sequences, indicates a proximal subaqueous depositional environment. The origin of the turbidites is from meltwater bottom-currents from subglacial tunnel-mouth outlets. They represent the common turbiditic bottom-currents as reported by Brodzikowski & van Loon (1991) and Mackiewicz et al. (1984). Their pulse-like appearance, documented by the intercalated diamictite beds, is indicative of seasonal or diurnal current strength/activity (Church & Gilbert 1975).

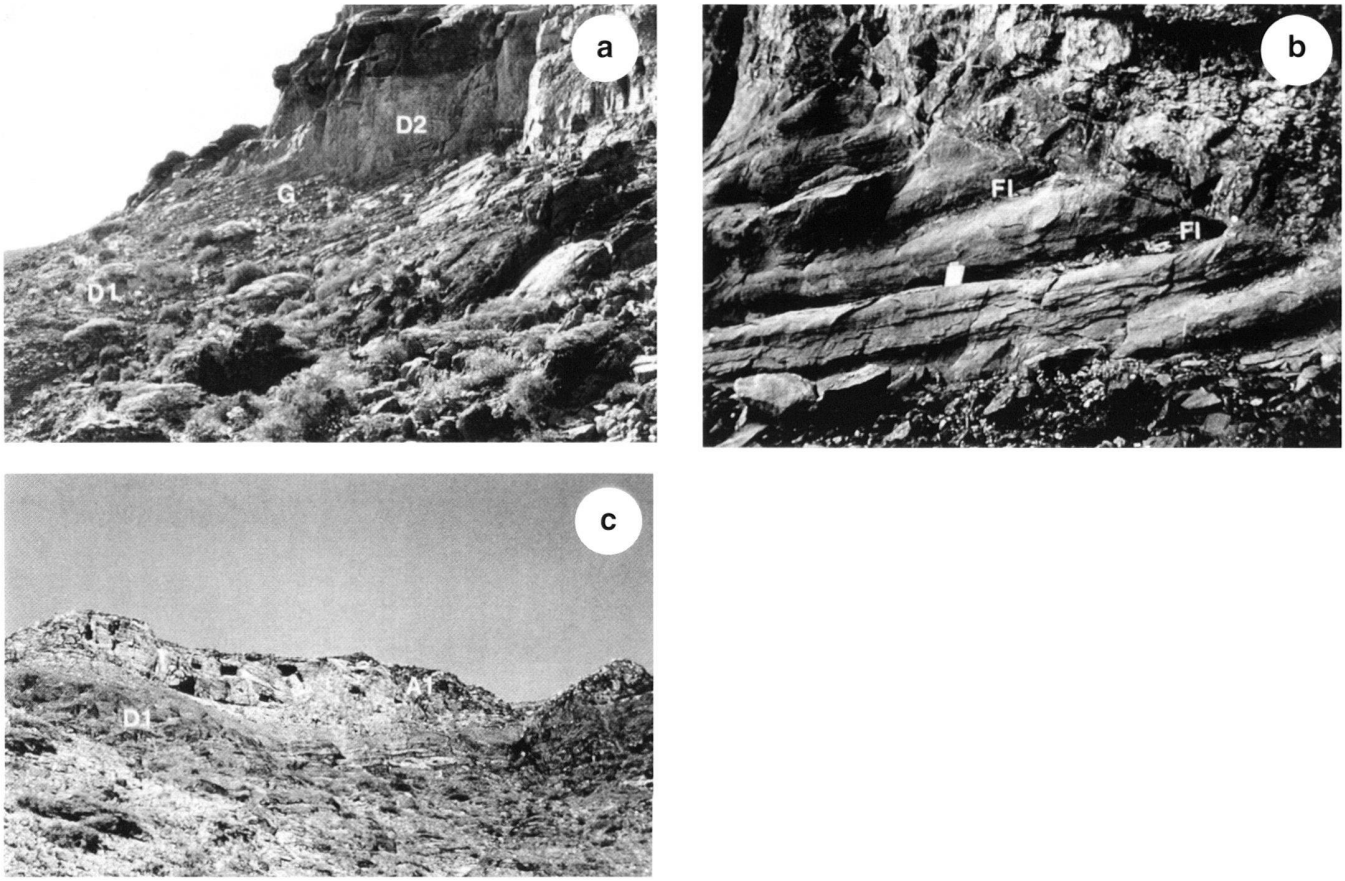

Fig. 7. Outcrop photographs: a) Gilbert delta showing increasing foreset dip angle from right to left. b) Detailed view of alternating foreset layers of sand - and dark silt (Fl), probably the result of diurnal current variations. The top is erosively overlain by diamictite D2. c) Channel A1 with giant foresets (alternate bars) of 25 m height. The channel is over 1.5 km wide and 35 m deep and is cut into the diamictite D1 of the distal glaciomarine facies association.

Terminoglacial deltaic system

Gilbert delta facies association

Description: The northern part of the sandstone channel (C: green in Fig. 3b) at the top of diamictite D1 can be traced towards the N where it forms large-scale foresets with a height of up to 15 m (G in Fig. 3a, b). The foreset angle steepens from about 20° in the proximal to 30° in the distal part (Fig. 7a). The sandstone foresets alternate with purple siltstone (Fl) layers (Fig. 7b). Each foreset consists of mm to cm thick layers of coarse sandstone which are sometimes slumped and displaced by small-scale normal faults. The contact with the overlying diamictite D2 is sharp and erosive, and the topsets are missing.

Interpretation: The steep, large-scale foresets were the result of downslope avalanching of loose clastic material as in a Gilbert delta. The transport mechanism was a traction current derived from a constant source. A high sedimentation rate led to oversteepening of the accumulated sediments and resulted in slumps and micro-faults. The preserved foreset height of 15 m represents a minimum water depth. The rhythmic alternation of sandstone and siltstone foresets in a near-glacial Gilbert delta was interpreted by Mastalerz (1990) as indicating diurnal oscillations of flow. The sandstones, therefore, reflect sedimentation under high meltwater discharge due to intense ablation caused by elevated daytime temperatures. At night, freezing resulted in lower stream discharge and sediment supply to the slipface, so that deposition from suspension dominated. The same pulsating current activity was also observed in the turbidite and channel sandbody facies association.

Rhythmite facies association

Description: Laterally and at the same stratigraphic level as the Gilbert Delta, a 2 m thick grey-green rhythmically-laminated siltstone (R in Fig. 3c) consisting of thin dark clay and thicker grey-green silt layers is present. The flat non-erosive base of this facies association is overlain mainly by Fl which shows occasional slumping. Many outsized clasts (<30 cm) pierce and

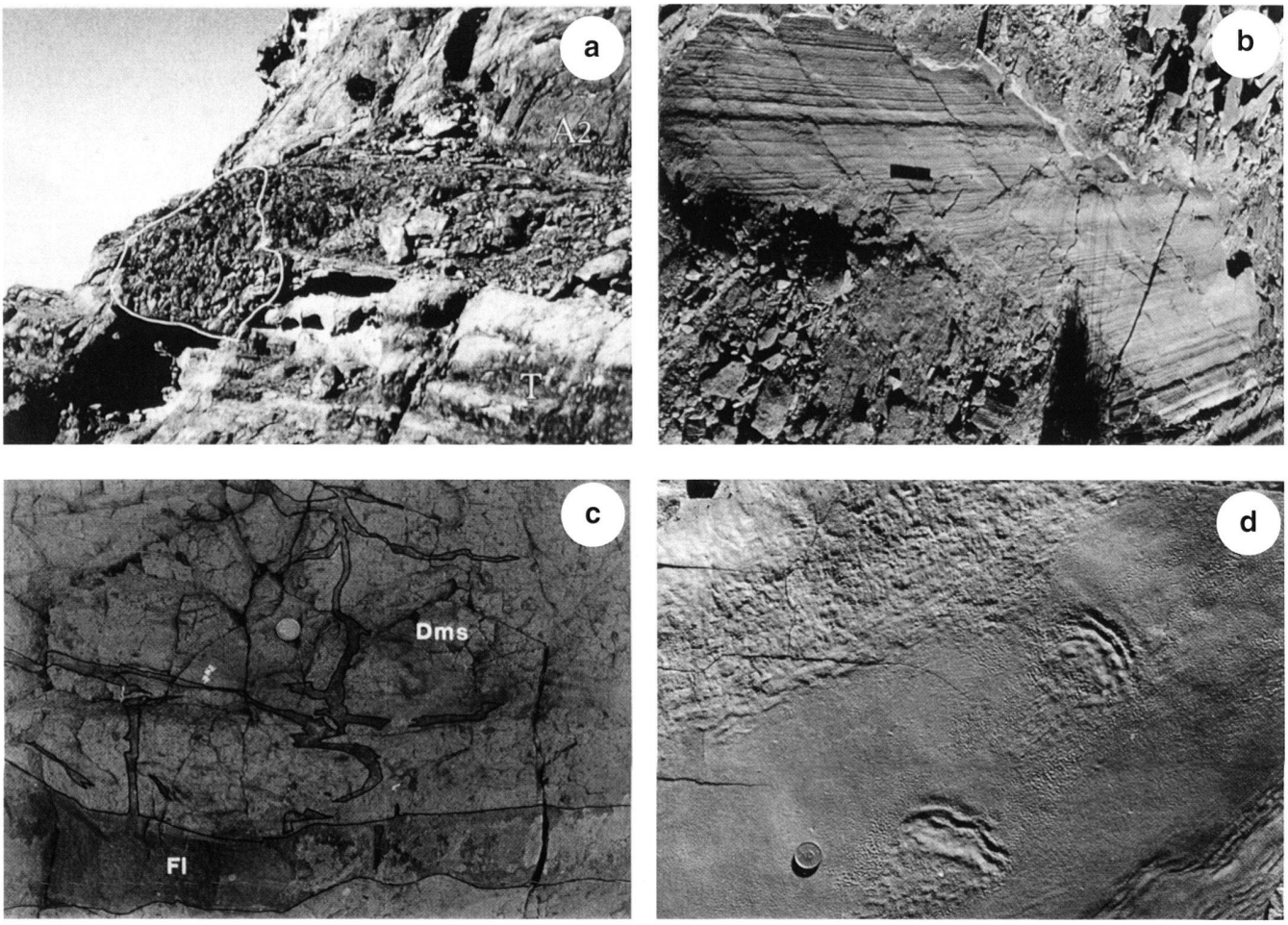

Fig. 8. Outcrop photographs: a) Marine glacial, tunnel-mouth deposit. The outlined circular channel-fill (2.5 m) of coarse breccia forms positive relief on top of the turbidite bed (T). This submarine esker is overlain by a thin layer of Dmm (not visible) and topped by the distributary channel A2.
b) Glacial striations on channel C1. Grooves are mm-cm deep with length of up to 30 m. Note pencil for scale. c) Compressed and sheared stratified diamictite (Dms) underneath glacial striations (Fig. 2; Profile A 95 m). Several clastic dikes, originating from the dark siltstone channel (Fl), were injected upward into the diamictite . The dike to the right of the coin (1.5 cm) is sheared whereas the one farther to the left shows no deformation. d) Cast of ice-made skip marks and runzelmarks, immediately overlying glacial striations.

cause downward bending of laminae. Scattered, up to 5 cm thick, sheet-like faintly graded sandstone (Sg) beds and some small (0.5–4 cm thick and 10–100 cm wide) graded sandstone (Sg) channels and gravel stringers are also found. The top 50 cm of this facies association show an increasing number of graded small-scale sandstone channels as well as an increasing sand content in the siltstone laminae. This coarsening-upward leads to a gradual transition into the overlying diamictite (Fig. 6d).

Interpretation: Even though the rhythmic layering gives an impression of varves, these sediments are most likely fine grained turbidites. This interpretation is supported by the occurrence of numerous graded turbiditic sandstone channels in the upper part of the unit. Taking into account that a Gilbert delta is found at the same stratigraphic level, these rhythmites are thought to represent deltaic bottomsets (Brodzikowski & van Loon, 1991) of another delta to the south, rather than varves. The coarsening-upward trend may either be due to an increase of current strength or to delta front progradation. During deposition of the turbidites/rhythmites there was a constant rain-out from icebergs (dropstones) indicating that the glacier reached the sea.

Limestone facies association

Description: In the uppermost 50 cm of the rhythmites, several cm to dm thick micritic to sandy, graded limestone (Lg) beds with scarce coccoid cyanobacterial cells are found. They are

deformed by the impact of dropstones (Fig. 5d). The <40 cm thick micritic fetid limestone which rests on top of the rhythmites is deformed by numerous slumps and synsedimentary faults. It shows a stongly negative carbon isotopic signature of –4.62‰.

Interpretation: The coccoid cyanobacterial remains are identical to those found in limestones of the distal glaciomarine deposits. Dropstones deforming these limestones beds are an unequivocal proof of cyanobacterial growth in a glacial environment. Similar microbial stromatolites are described from the glacial Proterozoic Stoer Group by Davison & Hambrey (1996).

Subglacial system

Marine glacial tunnel-mouth facies association

Description: Only one example of this facies association was found, on top of diamictite D2 (Fig. 3b) where it forms a linear channel with a nearly round cross-section. The channel has a diameter of 2.5 m transverse to the palaeoflow-direction and is filled by a poorly-sorted clast-supported slightly graded conglomerate (Cg). Half of this channel is eroded into an underlying turbidite channel, the rest forms positive relief (Fig. 8a). On both sides of this channel fill on top of the turbidite channel a pebbly conglomeratic wedge was deposited. A 2 m thick flat sheet-like massive matrix-supported diamictite (Dmm) bed of the rain-out diamictite facies association overlies the turbidite channel as well as the conglomeratic channel and wedges.

Interpretation: The coarse-grained lithofacies, positive relief and linear shape of this channel fill as well as its association with turbidite deposits and rain-out diamictites are indicative of a subaqueous glacial tunnel-mouth deposit. According to Brodzikowski & van Loon (1991) the coarse, poorly sorted infill of a tunnel-mouth deposit is the result of successive surges that may erode the top part of the previously deposited layer and therefore lead to a predominance of coarse-grained material.

Glacial striations facies association

Description: Glacial striations (Fig. 8b) occur in the upper third of the proximal glaciomarine deposits (Fig. 2: Profile A: 68 m, 95 m and 105 m) on and in channel C1 (Fig. 3b) and turbidites (Fig. 2: Profile B: 142 m), respectively. The mm to cm deep grooves are carved into a sandstone and the longest measure at least 30 m. The striations are oriented NW-SE, i.e. in the general flow direction. The diamictite layers (Dms) overlying the striae within channel C1 (Fig. 2: Profile A 95 m) are sheared and disrupted by numerous small-scale dykes which were injected upwards from an enclosed siltstone channel (Fig. 8c).

The striations on top of the uppermost large-scale channel sandbody (C1 in Fig. 2; Fig. 8b) are not associated with deformed sediments. A light, 1 cm thick finely-laminated silt/clay (Fl) layer covers the striations and shows runzelmarks, as well as ice-made skip marks (Fig. 8d) similar to those described by Dionne (1985) from a tidal platform of an estuary with seasonal ice.

Interpretation: Small-scale dykes similar to those found in the diamictites were ascribed by Dreimanis & Rappol (1997) to subglacial deformation. The coexistence of sheared and undeformed dykes within the same diamictite clearly indicates overconsolidation and multiple shearing caused by the overriding glacial ice.

The silt layer covering the striations on top of channel sandbody C1 was deposited after the retreat of the glacier ice in very shallow water as indicated by the ice-made skip marks and in combination with strong winds generating the runzelmarks (Häntzschel & Reineck 1968; Reineck 1969) .

Ice front system

Fluvial facies association

Description: Two kinds of channel fills occur in this facies association, with both ranging from 600 to 1500 m in width and from 15 to 35 m in depth. The first type (C1, C2) consists of occasional graded conglomerates (Cg) at the base overlain by vertically stacked dune cosets (Sc) (Fig. 2, Profile A: 73–105 m, Profile C: 145–170 m) and current ripples in the uppermost 2 m. Except for its greater width and coarser grain size this channel fill is similar to the channel sandstones found in the proximal glaciomarine deposits. A general fining-upward trend occurs in each of these channel fills. Glacial striations and diamictites were found within and on top of channel C1.

Channels of the second type (A1, A2) were found in only two locations (Fig. 3a, b, c). Both channels have erosive bases and a stacked trough cross-bedded sandstone unit (Sc) at their base. This is followed by up to 25 m thick giant, planar, avalanche foresets of 2-D bedforms (Fig. 7c). Rarely, dunes (Sc) can be observed migrating down the slipface. Channel A1 consists of a clay-free, orange to ochre arkose similar to that of all other channel sandbodies. In contrast, A2 is made up of a clay-rich arkose of maroon to brown colour similar to the matrix of the diamictites.

Interpretation: The large channel size as well as the infill of mostly cross-bedded sandstones, the fining-upward trend and current ripples in the uppermost part of the infill of the first channel type (C1, C2) are typical for a low sinuosity braided river (Nemec, 1992) or a sandy braided river (Cant & Walker 1976). However, planar cross-bedding which is a typical element in these river types is very scarce. The occurrence of glacial striae within and on top of these channel deposits and their association with diamictites suggests deposition within the limits of a dynamic glacier front.

Similar giant bedforms as found in the second channel type (A1, A2) were described by McCabe (1977) as alternate bars in a distributary channel of a delta. Such giant foresets are characteristic of large rivers similar to the modern Mississippi (McCabe 1977). They imply that large amounts of meltwater

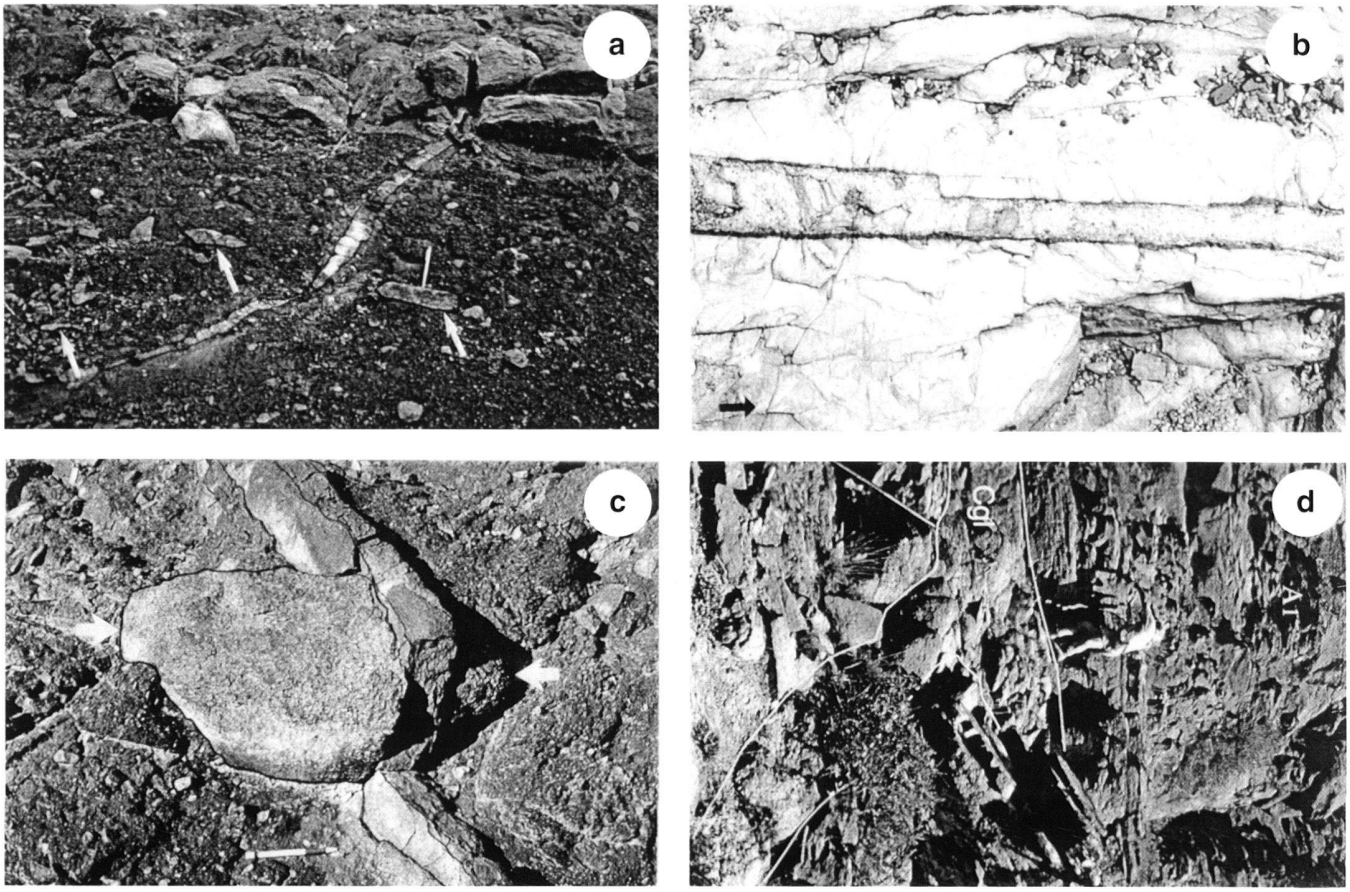

Fig. 9. Outcrop photographs: a) Small clastic dike injected into a Dmm . Clast long-axes (arrows) show a clear orientation suggesting a lodgement till diamictite (pencil for scale). b) Clastic dike with poorly sorted fill material. Arrow points stratigraphically up. Scale bar is 20 cm. c) Clastic dike crosscutting a large crystalline clast (arrows). d) One of the few places where the origin of a clastic dike is visible. This approximately 80 cm wide dike originates from a conglomeratic channel fill.

with a variable suspension load must have been released by the glacier as indicated by the different clay content of channel A1 and A2 sandstones.

Subaerial non glacial system

Scree facies association

Description: The stratigraphically lowest sediments, found only in the western part (Fig. 3a) of the study area, consist of a dark purple clastic sequence, measuring approximately 5.5 m in thickness. At the base of the sequence is a pebbly graded breccia (Bg) 0.5 m thick. The angular to subangular clasts are derived exclusively from the underlying crystalline basement (Sadh-Gneisses). The matrix consists of a subangular, rounded, clay-rich lithic arkose. The breccia is overlain by an approximately 30 cm thick bed of purple siltstone. The contact is sharp and slightly erosive. The thinly laminated siltstone (Fl) locally shows intercalations with more or less single grain sandstone laminae and minor soft sediment deformation. The siltstone is succeeded by an erosively based, wedge shaped, >2.5 m thick, massive, clast-rich diamictite (Dmc) with a purple silt to sand matrix (Fig. 4a). The angular to subrounded boulders consist almost entirely of Sadh-Gneiss and rare granitic and basic dyke rocks with an average diameter of 60 cm (max. 2 m). In the top of this sequence several gravel stringers occur where the first volcanic clast can be found. All these sediments were deposited at the base of a nearly vertical valley flank with a rugged surface.

Interpretation: If the surrounding sediments are taken into account, the graded breccia (Bg) covering the crystalline basement represents most probably a debris flow deposit. The laminated siltstones (Fl) and the silty sandstones (Sl) are the result of fluvial transport. The angular clasts of the clast-rich diamictite (Dcm), sourced almost exclusively from the directly underlying crystalline basement, indicate a local source and a short transport distance, which is typical for scree deposits. The sandstones overlying the diamictites show a decreasing grain size and include volcanic clasts suggesting a return to fluvial transport.

Discussion

Facies evolution and depositional processes

Tracing the lateral facies changes in continuous outcrops reveals the complete facies evolution within the Lower Member of the Mirbat Sandstone Formation. The palaeotopography of the crystalline basement within the study area is dominated by two north-south trending palaeovalleys (Fig. 10a). The larger valley, to the east, is at least 2 km wide and more than 150 m deep with a faulted eastern margin (Fig. 1, 10a). The smaller N-S trending palaeovalley is narrower and more U-shaped. The western side of this valley is marked by a small, U-shaped hanging valley. The rare outcrops of the palaeovalley floors reveal rough surfaces with a cm-.scale topography.

Subaerial-fluvial environment

The oldest sediments are exposed only in the small N-S trending palaeovalley where deposition began with subaerial scree deposits which accumulated along steep valley sides (Fig. 3a, 10a). The absence of a weathering profile together with a rugged cm-scale topography reveal the dominance of physical weathering. The scree deposits are overlain by 3 m of stacked fluviatile channel sandbodies consisting of silt-rich arkose containing outsized clasts of pink granites. These pink granites are not found locally in the present crystalline basement, and suggest fluviatile transport over at least several tens of kilometers.

Lower distal glaciomarine environment

Following deposition of the scree and fluvial deposits, the valley was flooded by rising sea-level (Fig. 10b), indicated by the deposition of rain-out diamictite facies association (D1) in a glacial environment. The common occurrence of isolated stacked channel sandbodies in the eastern part of the study area points to a nearby tunnel-mouth exit. The frequent slumps show the high instability of the sediments, possibly due to oversteepening of sediment accumulations and/or tectonic activity (Lash 1984; Young & Nesbitt 1985). Rain-out was the dominant sedimentation process, indicating that the glacier reached the sea. A pause in rain-out is indicated by the presence of two stromatolitic carbonate beds in the central part of the western photo panorama (Fig. 3b). However, turbidity currents prevailed during this pause as shown by the associated calciturbidites and siliciclastic turbidites.

In the uppermost meters of diamictite D1 there is a gradual increase of the clay content in the matrix and the glacially shaped, striated clasts show a distinct N-S orientation of their long axes (Fig. 9a). These are typical indicators for a lodgment till (Boulton & Deynoux 1981; Eyles et al. 1993; Menzies 1996). The succession shows the transition from rain-out to subglacial deposition. This glacial advance is marked in Figure 10f by the first pair of arrow heads. Moreover, sand wedge structures originating from a sandstone channel fill overlying the lodgment till are present (Fig. 9a). Their massive texture precludes a permafrost origin. This subglacial horizon is missing farther to the NW in the area of the future Gilbert delta due to the erosion of a large channel formed by a meltwater stream.

Terminoglacial deltaic environment

In the westernmost valley, a terminoglacial Gilbert delta (G) and its feeder channel (C: green in Fig. 3b) were deposited in the above mentioned erosive channel (Fig. 3b, 10c). During a later erosional event the upper part of the fluvial feeder channel infill was removed by another erosive channel which was then infilled initially by a Dmm and finally by dropstone-bearing turbidites interbedded with <50 cm thick Dmm beds (D and T respectively in Fig. 3b). This sequence is interpreted to indicate a transgression with constant rain-out from icebergs punctuated by turbiditic events. The pulsating occurrence of turbidity currents may be due to the same diurnal sediment supply pattern recognized in the Gilbert delta, or to seasonal changes in the sediment supply (Church & Gilbert 1975; Domack 1984; Eyles 1993).

Concomitant with the formation of the Gilbert delta, fine grained rhythmites (R) were deposited to the east of the crystalline ridge which separated more open water from the Gilbert delta (Fig. 10c). The stromatolites found in the uppermost part of the rhythmites indicate reduced sediment supply, allowing growth of cyanobacterial mats. The uppermost parts of the mats then were reworked into the overlying turbidite. The frequent dropstones demonstrate rain-out from icebergs and indicate that the glacier reached the sea.

Proximal glaciomarine, fluvial to subglacial environment

Unit D2 of the rain-out facies association was laid down on the erosional surface truncating the Gilbert delta and buries the remaining relief of the crystalline basement. This unit interfingers towards the east with the other deposits of the proximal glaciomarine environment. In the central part of D2 huge, 'flame-shaped' soft-sediment deformation features representing folded channels are present (Fig. 3a and 10d). These folds are thought to be the result of glaciotectonism because D2 is overlain by a subglacial tunnel-mouth deposit (Fig. 10d-inset, Fig. 8a).

The subglacial horizon of the tunnel-mouth deposit can be followed to the east where it forms the top of the strongly erosive large-scale distributary channel A1 and the smaller channel inbetween as shown in Fig. 10d. A large-scale dyke originating from the smaller channel extends more than 80 m downwards into the underlying diamictite (D1). The massive texture and sharp-bounded walls of this and numerous similar, large-scale neptunean dykes, together with the fact that they occasionally cut across boulders, preclude an ice-wedge origin (Fig. 9 b-d). Moreover, some of these dykes show soft sediment deformation and are cross-cut by undeformed dykes showing that the host sediment was not cemented during dyke injection. These observations demonstrate changes from brittle to ductile behaviour of the host rock. Gravity loading by the

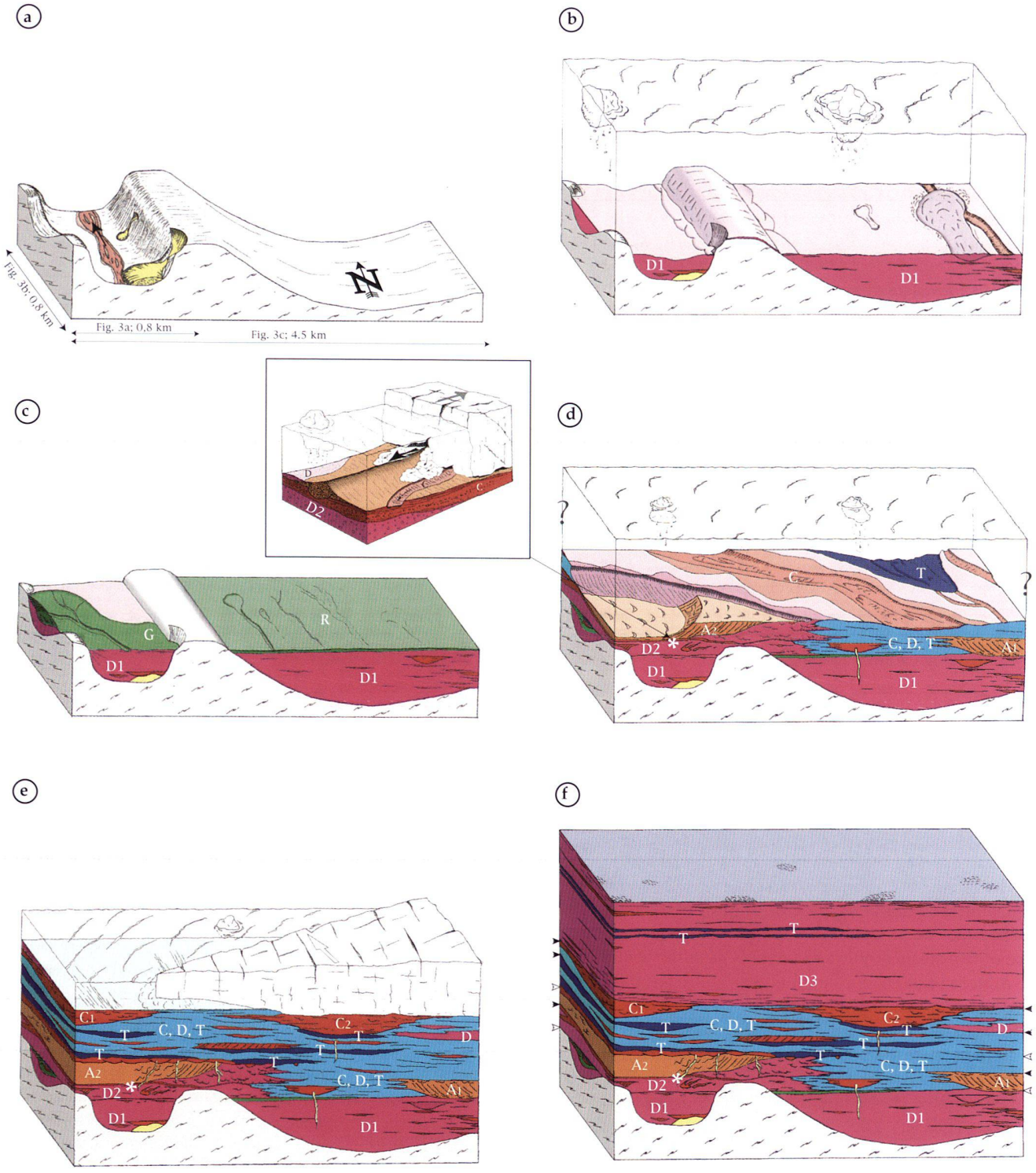

Fig. 10. Facies evolution and depositional processes observed in the study area. See text for discussion. Abbreviations as in Fig. 3. Arrow heads indicate palaeo-subglacial horizons and/or glacial retreats.

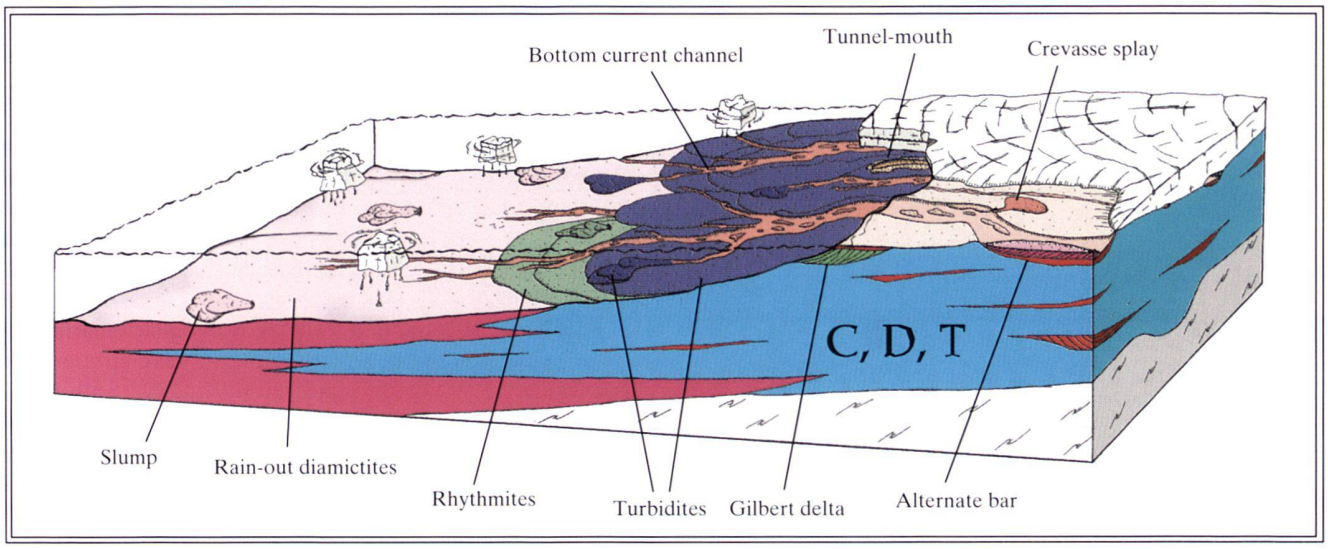

Fig. 11. General facies model of the Lower Member. (C, D, T): proximal glaciomarine deposits.

advancing glacier compacted the diamictites into rigid bodies (Lerche et al. 1997). High pressures that developed in the encased water-saturated channel sediments were released by downward injection of channel fill material into fractures in the host sediment. Pressure release due to the retreat of the glacier allowed the host sediment to deform as a ductile sediment. Cross-cutting relationships and displacement of dykes document tectonic activity during dyke formation which may be related to the rifting of the Abu Mahara Basin (Abed et al. 1993).

The observed succession of terminoglacial deltaic-, rain-out-, current dominated proximal glaciomarine and subglacial deposits indicates a transgression followed by a regression and glacier advance. The latter is marked in Figure 10f by the second pair of arrow heads.

In the west of the study area, the distributary channel A2 was laid down on top of the former subglacial surface (Fig. 10d). This almost E-W trending distributary channel reveals the transition to fluvial conditions and records another regression. This channel fill was then penetrated by numerous clastic dykes sourced from the overlying channel sandbody possibly as the result of glacial advance (Fig. 10f, third pair of arrow heads).

Following deposition of this fluvial sandstone, subaqueous conditions were re-established within the entire study area and proximal glaciomarine sediments were deposited. Rain-out diamictite, turbidite and channel sandbody facies associations occur in intimate vertical and lateral successions (Fig. 10d, C, D, T). Glacial striations found on the turbidite channel in the upper part of this system (Fig. 2 Profile A; 69 m) demonstrate another glacial advance (Fig. 10f, fourth pair of arrow heads). Glacial striations on the surface and within the fluvial channel (C1) and the associated runzelmarks record a regression and the last ice advance in the Lower Member (Fig. 10f, fifth pair of arrow heads).

Upper distal glaciomarine environment

Proximal glaciomarine and fluvial conditions give way to a distal glaciomarine environment as revealed by diamictite D3. The changing abundance of sandstone channels from high at the base to low in the middle and high again in the upper part of D3 indicates changing proximity to the glacial front as a result of a transgression and a following regression.

The regionally persistent thin stromatolitic limestone which directly overlies the glaciogenic deposits of the Mirbat Sandstone Formation (Fig. 10f) is equivalent to the cap dolostones found above numerous Late Proterozoic diamictites in Australia, West Africa and North America (Deynoux 1985; Eyles 1993) . It shows some of their characteristic attributes described for example by Kennedy et al. (2001) like a strongly negative carbon isotope signature, microbial lamination and domal structures as well as scarce barite crystal fans. However, other features frequently associated with cap carbonates like tube structures and abundant formerly aragonitic crystal fans are missing. This limestone reflects the end of the glacial conditions and the final glacial retreat in the Lower Member.

Conceptual facies model

The vertical succession of the depositional units together with their geometry permit reconstruction of a conceptual facies model of the Lower Member of the Mirbat Sandstone Formation illustrated in Figure 11. The model resembles that of

Brodzikowski & van Loon (1991) for the terminoglacial environment. Figure 11 shows an area with a floating ice sheet, which is the source of icebergs whose influence is most pronounced in the distal glaciomarine environment. The proximal glaciomarine environment is characterised by mass flow deposits and subaqueous channel sandstones deposited by low temperature, highly sediment-laden underflows. Closely associated with the proximal glaciomarine environment are proglacial deltaic deposits and rhythmites which are interpreted as distal turbidites. After retreat of the glacier a terminoglacial fluviatile plain develops between the ice front and the coast (schematically shown on Fig. 11). This fluviatile plain is then overridden by the next glacial advance. Glacial loading caused overpressures in the channel sandstones and injection of sandstone dykes into the underlying proximal glaciomarine sediments. The next transgression (relative sea-level rise) resulted in the deposition of further proximal glaciomarine or distal glaciomarine deposits. These relative sea-level fluctuations may have had several causes. Although regional tectonics is indicated by the clastic dykes, glacioeustatism as well as glacioisostasy may have also played a role. Determining the dominating process for the sea-level fluctuations would require studies of Late Proterozoic glacial sediments from other areas in Arabia.

The evidence of huge meltwater streams, diurnal variations of meltwater in combination with short term advances and retreats of the ice front suggest a temperate glacier, typical for the Late Proterozoic glaciations according to Eyles et al. (1993). This is supported by paleomagnetic data indicating deposition of the Mirbat Sandstone Formation at about 10°N (Kempf et al. 2000). This result is compatible with a recent reconstruction of the Panotian supercontinent at 545 Ma showing low palaeolatitudes for the Arabian shield (Dalziel 1997) . Thus the Mirbat Sandstone Formation represents yet another example of these enigmatic low-latitude Neoproterozoic glacial successions which have been interpreted as evidence for a snowball Earth (see review by Hoffman & Schrag 2002). This provocative hypothesis invokes a planet which was completely covered by ice, followed by rapid melt-back after the CO_2-level had climbed back to cause a large enough greenhouse effect to melt the ice. This scenario rests less on the study of the glacials themselves than on detailed sedimentological and carbon-isotope investigations of the carbonates which both underlie and "cap" the glacial successions. The hypothesis implies that during the snowball phase the hydrological cycle is shut down. However, the Mirbat Sandstone Formation reveals, as discussed above, dynamic conditions and a functioning hydrologic cycle. According to Condon et al. (2002) such conditions are characteristic of many Neoproterozoic glacial deposits and imply that the seas were not totally frozen.

Conclusions

The Lower Member of the Mirbat Sandstone Formation contains a high-resolution record allowing reconstruction of depositional processes and palaeoenvironment and development of a conceptual facies model of a highly complex glaciomarine setting of a Neoproterozoic glaciation. As pointed out by Eyles et al. (1985) and others, the reconstruction of a glaciomarine palaeoenvironment is only possible if one 'investigates on a broad regional scale using multivariate basin analysis techniques in which lithofacies sequences, stratigraphic association and geometry are identified'. The proximal glaciomarine facies particularly is marked by a non-layer cake stratigraphy (Eyles et al. 1985) with rapid lateral and vertical facies changes. Detailed analysis of facies associations and their geometrical relationships lead to the conclusion that apparently fluvial sandstone channel fills actually represent subaqueous traction current deposits within the proximal glaciomarine environment. This is in contrast to most other ancient examples described in the literature, which report turbidite channel sandstones from this environment. Traction current deposits producing fluvial-like channel deposits have been mentioned by Brodzikowski & van Loon (1991) and Eyles et al. (1985). In this paper the bottom-currents are thought to represent cold and sediment-laden meltwater streams.

The occurrence of stromatolites within the glacial succession indicates decreased activity of meltwater bottom-currents and rain-out deposition allowing growth of microbial mats. These stromatolites may be the equivalents of algal mats found in recent Antarctic lakes (Wharton 1994), rather than reflecting warm water conditions, thereby circumventing the 'dolomite/tillite paradox' (Eyles 1993). The detrital composition of the Mirbat Sandstone Formation consisting of basement detritus only, as well as the predominance of rounded clasts and common faceted and striated glacial pebbles record erosion and transport by wet-based continental glaciers and rivers prior to deposition in the sea. In addition, the sedimentary architecture shows the synchronous deposition of glacial, fluvial and marine facies (Fig. 10f, 11). The consistency of the observations reveals that the Neoproterozoic seas were not totally frozen, but that in equatorial latitudes there was open water as suggested by the "loophole model" (Hyde et al. 2000, Runnegar, 2000).

Acknowledgements

This paper represents part of the senior author's Ph.D-thesis carried out at the University of Berne. The authors thank Dr. Hilal Al Azri, Director General of Minerals, Ministry of Commerce and Industry of the Sultanate of Oman for help and support. We thank M. Deynoux for his efforts in reviewing an earlier version of this manuscript. The Eclogae reviewers Andy Knoll and Graham Shields are thanked for thorough reviews and constructive comments. Finally we thank Steve Burns for his help with the English.

REFERENCES

ABED, A. M., MAKHLOUF, I. M., AMIREH, B. S. & KHALIL, B. 1993: Upper Ordovician glacial deposits in southern Jordan. Episodes 16, 316–328.

BOULTON, G. S. & DEYNOUX, M. 1981: Sedimentation in glacial environments and the identification of tills and tillites in ancient sedimentary sequences. Precambr. Res. 15, 397–422.

BRINER, A. 1997: The anatomy of a Late Proterozoic continental margin at mid-crustal level: rapid crust formation and accretion in the Dhofar (Sultanate of Oman) portion of the Arabian shield. PhD-thesis, University of Berne.

BRASIER, M., MCCARRON, G., TUCKER, R., LEATHER, J., ALLEN, P. & SHIELDS, G. 2000: New U-Pb zircon dates for the Neoproterozoic Ghubrah glaciation and for the top of the Huqf Supergroup, Oman. Geology 28, 175–178.

BRODZIKOWSKI, K. & VAN LOON, A. J. 1991: Glacigenic Sediments. Elsevier, Amsterdam, 674 pp.

CANT, D. J. & WALKER, R. G. 1976: Development of a braided-fluvial facies model for the Devonian Battery Point Sandstone, Quebec. Canad. J. Earth Sci. 13, 102–119.

CHURCH, M. & GILBERT, R. 1975: Proglacial fluvial and lacustrine environments. In: Glaciofluvial and glaciolacustrine sedimentation (Ed. by JOPLIN, A. V. & MCDONALD, B. C.). Spec. Publ. Soc. econ. Paleont. Mineral. 25, 22–100.

DALZIEL, I. W. D. 1997: Neoproterozoic-Palaeozoic geography and tectonics: Review, hypothesis, environmental speculation. Bull. Geol. Soc. Amer. 109, 16–42.

DAVISON, S. & HAMBREY, M. J. 1996: Indications of glaciation at the base of the Proterozoic Stoer Group (Torridonian), NW Scottland. J. geol. Soc. 153, 139–149

DEYNOUX, M. 1985: Terrestrial or waterlain glacial diamictites? Three case studies from the late Precambrian and the late Ordovician glacial drifts in West Africa. Palaeogeogr. Palaeoclimatol. Palaeoecol. 51, 97–141.

DIONNE, J.-C. 1985: Formes, figures et faciès sédimentaires glaciels des estrans vaseux des régions froides. Palaeogeogr. Palaeoclimatol. Palaeoecol. 51, 415–451.

DOMACK, E. W. 1983: Facies of Late Pleistocene glacial-marine sediments on Whidbey Island, Washington: an istostatic glacial-marine sequence. In: Glacial-marine sedimentation (Ed. by Molina, B. F.), pp. 535–570. Plenum Press, New York.

– 1984: Rhythmically bedded glaciomarine sediments on Whidbey Island, Washington. J. sediment. Petrol. 54, 589–602.

DREIMANIS, A. 1979: The problems of waterlain tills. In: Moraines and varves (Ed. by Schlüchter, C. H.), pp. 167–177. Balkema, Rotterdam,

DREIMANIS, A. & RAPPOL, M. 1997: Late Wisconsian sub-glacial clastic intrusive sheets along Lake Erie bluffs, at Bradtville, Ontario, Canada. Sediment. Geol. 111, 225–248.

EVANS, D. A. D. 2000: Stratigraphic, geochronological, and paleomagnetic constraints upon the Neoproterozoic climatic paradox. Amer. Jour. Science 300, 347–433.

EYLES, N. 1977: Late Wisconsin glacitectonic structures and evidence of postglacial relict permafrost in north-central Newfoundland. Canad. J. Earth Sci. 14, 2797–2806.

– 1993: Earth's glacial record and its tectonic setting. Earth-Sci. Rev. 35, 1–248.

EYLES, N., EYLES, C. & MIALL, A. D. 1983: Lithofacies types and vertical profile models; an alternative approach to the description and environmental interpretation of glacial diamictite and diamictite sequences. Sedimentology 30, 393–410.

EYLES, N., EYLES, C. & MIALL, A. D. 1985: Models of glaciomarine sedimentation and their application to the interpretation of ancient glacial sequences. Palaeogeogr. Palaeoclimatol. Palaeoecol. 51, 15–84.

EYLES, C. H., EYLES, N. & FRANCA, A. B. 1993: Glaciation and tectonics in an active intracratonic basin: the Late Palaeozoic Itararé Group, Paranà Basin, Brazil. Sedimentology 40, 1–25.

GASS, G., RIES, A. C., SHACKLETON, R. M. & SNEWING, J. D. 1990: Tectonics, geochronology and geochemistry of the Precambrian rocks of Oman. In: The Geology and Tectonics of the Oman Region (Ed. by ROBERTSON, A. H. F., SEARLE, M. P. & RIES, A.), Spec. Publ. Geol. Soc. London 49, 585–599.

GORIN, G. E., RACZ, L. G. & WALTER, M. R. 1982: Late Precambrian-Cambrian sediments of Huqf Group, Sultanate of Oman. Bull. amer. Assoc. Petroleum Geol. 66, 2609–2627.

HÄNTZSCHEL, W. & REINECK, H. E. 1968: Fazies-Untersuchungen im Hettangium von Helmstedt (Niedersachsen). Mitt. geol. Staatsinst. Hamb. 37, 5–39.

HELAL, A. H. 1964: On the occurrence and stratigraphic position of Permo-Carboniferous tillites in Saudi Arabia. Geol. Rdsch. 54, 193–207.

HOFFMAN, P. F., KAUFMAN, A. J., HALVERSON, G. P. & SCHRAG, D. P. 1998: A Neoproterozoic snowball earth. Science 281, 1342–1346.

HOFFMAN, P. F. & SCHRAG, D. P. 2002: The snowball Earth hypothesis: testing the limits of global change. Terra Nova 14, 129–155.

HYDE, W. T., CROWLEY, T. J., BAUM, S. K. & PELTIER, W. R. 2000: Neoproterozoic "snowball Earth" simulations with coupled climate/ice-sheet model. Nature 405, 425–429.

KELLERHALS, P. 1993: Igneous petrology of the Mirbat Complex and facies analysis of the Mirbat Sandstone Formation (Middle and Upper Member). Unpubl. MSc-thesis, University of Berne, 96pp.

– 1998: Ice age related erosional and depositional processes: examples from the late Proterozoic and Quaternary, Sultanate of Oman. Ph.D. thesis, University of Berne, 97pp.

KEMPF, O., KELLERHALS, P., LOWRIE, W. & MATTER, A. 2000: Paleomagnetic directions in Late Precambrian glaciomarine sediments of the Mirbat Sandstone Formation, Oman. Earth and planet. Sci. Lett. 175, 181–190.

KENNEDY, M. J., CHRISTIE-BLICK, N. & SOHL, L. E. 2001: Are Proterozoic cap carbonates and isotopic excursions a record of gas hydrate destabilization following Earth's coldest intervals? Geology 29, 443–446.

KIRSCHVINK, J. L. 1992: Late-Proterozoic low-latitude global glaciation: the snow-ball earth. In: The Proterozoic Biosphere (Ed. by SCHOPF, J.W. & KLEIN, C.), pp 51–52. Cambridge University Press, Cambridge.

KLEIBER, H.-P. 1993: Igneous petrology of the Mirbat Complex and facies analysis of the Mirbat Sandstone Formation (Lower Member). Unpubl. MSc-thesis, University of Berne, 106pp.

KRUCK, W. & THIELE, J. 1983: Late Palaeozoic glacial deposits in the Yemen Arab Republic. Geol. Jb. [Reihe B] 46, 3–29.

LASH, G. G. 1984: Density-modified grain-flow deposits from an early Paleozoic passive margin. J. sediment. Petrol. 54, 557–562.

LEATHER, J. 2001: Sedimentology of the glaciomaine sediments of the Neoproterozoic Ghadir Manqil Formation, Jebel Akhdar, Oman. Int. Conf. Geology Oman, Abstract Vol. p. 54.

LERCHE, I., YU, Z., TØRDBAKKEN, B. & THOMSEN, R. O. 1997: Ice loading effects in sedimentary basins with reference to the Barents Sea. Marine Petr. Geol. 14, 277–338.

LEVELL, B. K., BRAAKMANN, J. H. & RUTTEN, K. W. 1988: Oil-bearing sediments of the Gondwana glaciation in Oman. Bull. amer. Assoc. Petroleum Geol. 72, 775–796.

LOOSVELD, R., BELL, A. & TERKEN, J. 1996: The tectonic evolution of Interior Oman. GeoArabia 1, 28–51.

MACKIEWICZ, N. E., POWELL, R. D., CARLSON, P. R. & MOLINA, B. F. 1984: Interlaminated ice-proximal glacimarine sediments in Muir Inlet, Alaska. Marine Geol. 57, 113–147.

MASTALERZ, K. 1990: Diurnally and seasonally controlled sedimentation on a glaciolacustrine forset slope: an example from the Pleistocene of eastern Poland. In: Coarse-grained deltas (Ed. by COLLELA, A. & PRIOR, P. D.), Spec. Publ. Int. Ass. Sediment. 10, 297–309.

MCCABE, P. J. 1977: Deep distributary channels and giant bedforms in the Upper Carboniferous of the Central Pennines, northern England. Sedimentology 24, 271–290.

MCCLURE, H. A. 1978: Early Palaeozoic glaciation in Arabia. Palaeogeogr. Palaeoclimatol. Palaeoecol. 25, 315–326.

– 1980: Permian-Carboniferous glaciation in the Arabian Peninsula. Bull. geol. Soc. Amer. 91, 707–712.

MENZIES, J. 1996: Past glacial environments, sediments, forms and techniques. Butterworth-Heinemann, Oxford, London, 598 pp.

NEMEC, W. 1992: Depositional controls on plant growth and peat accumulations in a braid plain delta environment: Helvetiafjellet Formation (Barremian-Aptian), Svalbard. In: Controls on the Distribution on Quality of the Cretaceous Coals (Ed. by MCCABE, P. J. & TOTMAN PARRISH, J.), Boulder. Spec. Pap. geol. Soc. Amer. 267, 209–226.

PLATEL, J. P., ROGER, J., PETERS, T., MERCOLLI, I., KRAMERS, J. D. & LE MÉTOUR, J. 1992: Geological map of Salalah, Sheet NE 40–09, 1:250'000 with explanatory notes. Directorate General of Minerals, Oman Ministry of Petroleum and Minerals.

QIDWAI, H. A., KHALIFA, M. I. & BA-MKHALIF, K. A. 1988: Evidence of Permo-Carboniferous glaciation in the basal Murbat Sandstone Formation, Southern Region, Sultanate of Oman. J. Petrol. Geology 11, 81–88.

REINECK, H.-E. 1969: Die Entstehung von Runzelmarken. Senkenbergiana Marit. 1, 165–168.

RUNNEGAR, B. 2000: Loophole for snowball Earth. Nature 405, 403–404.

RUST, B. R. & ROMANELLI, R. 1975: Late Quaternary subaqueous outwash deposits near Ottawa, Canada. In: Glaciofluvial and glaciolacustrine sedimentation (Ed. by JOPLIN, A. V. & MCDONALD, B. C.). Spec. Publ. Soc. econ. Paleont. Mineral. 25, 177–192.

TUCKER, M. E. 1986: Formerly aragonitic limestones associated with tillites in the Late Proterozoic of Death Valley, California. J. sediment. Petrol. 56, 818–830.

VASLET, D. 1990: Upper Ordovician glacial deposits in Saudi Arabia. Episodes 13, 147–160.

WHARTON, R. A. J. 1994: Stromatolitic mats in Antarctic lakes. Kluwer Academic Publishers, Dordrecht, Boston, London, 471 pp.

WRIGHT, V. P., RIES, A. C. & MUNN, S. G. 1990: Intraplatformal basin-fill deposits from the Infracambrian Huqf Group, east Central Oman. In: The Geology and Tectonics of the Oman Region (Ed. by ROBERTSON, A.H.F., SEARLE, M. P. & RIES, A.C.). Spec. Publ. geol. Soc. London 49, 601–616 .

WÜRSTEN, F. 1994: The Precambrian crystalline basement of Salalah. Ph.D-thesis, University of Berne, 261pp.

YOUNG, G. M. & NESBITT, H. W. 1985: The Gowganda Formation in the southern part of the Huronian Outcrop Belt, Ontario, Canada: Stratigraphy, depositional environments and regional tectonic significance. Precambr. Res. 29, 265–301.

Manuscript received July 27, 2001
Revision accepted September 30, 2002